Multiple toxins and a protease contribute to the aphid killing ability of Pseudomonas fluorescens PpR24

Paliwal, D. ORCID: https://orcid.org/0000-0002-6891-0778, Rabiey, M., Mauchline, T. H., Hassani-Pak, K., Nauen, R., Wagstaff, C. ORCID: https://orcid.org/0000-0001-9400-8641, Andrews, S. ORCID: https://orcid.org/0000-0003-4295-2686, Bass, C. and Jackson, R. W. (2024) Multiple toxins and a protease contribute to the aphid killing ability of Pseudomonas fluorescens PpR24. Environmental Microbiology, 26 (4). e16604. ISSN 1462-2920 doi: 10.1111/1462-2920.16604 Available at https://centaur.reading.ac.uk/115559/

Received: 20 September 2023 | Accepted: 23 February 2024

DOI: 10.1111/1462-2920.16604

BRIEF REPORT

ENVIRONMENTAL MICROBIOLOGY

Multiple toxins and a protease contribute to the aphid-killing ability of *Pseudomonas fluorescens* PpR24

Deepa Paliwal[1] | **Mojgan Rabiey**[2] | **Tim H. Mauchline**[3] | **Keywan Hassani-Pak**[4] | **Ralf Nauen**[5] | **Carol Wagstaff**[6] | **Simon Andrews**[1] | **Chris Bass**[7] | **Robert W. Jackson**[1,8]

[1]School of Biological Sciences, University of Reading, Reading, UK

[2]School of Life Sciences, University of Warwick, Coventry, UK

[3]Sustainable Soils and Crops, Rothamsted Research, Harpenden, UK

[4]Intelligent Data Ecosystems, Rothamsted Research, Harpenden, UK

[5]Bayer Crop Science, Cambridge, UK

[6]School of Chemistry, Food and Pharmacy, University of Reading, Reading, UK

[7]University of Exeter, Penryn, UK

[8]School of Biosciences and Birmingham Institute of Forest Research, University of Birmingham, Birmingham, UK

Correspondence
Robert W. Jackson, School of Bioscineces and Birmingham Institute of Foresr Research, University of Birmingham, Edgbaston, Birmingham, B15 2TT, UK.
Email: r.w.jackson@bham.ac.uk

Mojgan Rabiey, School of Life Sciences, University of Warwick, Gibbet Hill Road, Coventry, CV4 7AL, UK.
Email: mojgan.rabiey@warwick.ac.uk

Funding information
University of Reading; Bayer Crop Science; BBSRC, Grant/Award Number: BB/P006272/1; UKRI, Defra, and the Scottish Government, under the Strategic Priorities Fund Plant Bacterial Diseases programme, Grant/Award Number: BB/T010568/1; BBSRC funded Growing Health, Grant/Award Number: BB/X010953/1; Soils to Nutrition, Grant/Award Number: BBS/E/C/000I0310; Institute Strategic Programmes; NERC Biomolecular Analysis Facility Liverpool via award, Grant/Award Number: NBAF794

Abstract

Aphids are globally important pests causing damage to a broad range of crops. Due to insecticide resistance, there is an urgent need to develop alternative control strategies. In our previous work, we found *Pseudomonas fluorescens* PpR24 can orally infect and kill the insecticide-resistant green-peach aphid (*Myzus persicae*). However, the genetic basis of the insecticidal capability of PpR24 remains unclear. Genome sequencing of PpR24 confirmed the presence of various insecticidal toxins such as Tc (toxin complexes), Rhs (rearrangement hotspot) elements, and other insect-killing proteases. Upon aphids infection with PpR24, RNA-Seq analysis revealed 193 aphid genes were differentially expressed with down-regulation of 16 detoxification genes. In addition, 1325 PpR24 genes (542 were upregulated and 783 downregulated) were subject to differential expression, including genes responsible for secondary metabolite biosynthesis, the iron-restriction response, oxidative stress resistance, and virulence factors. Single and double deletion of candidate virulence genes encoding a secreted protease (AprX) and four toxin components (two TcA-like; one TcB-like; one TcC-like insecticidal toxins) showed that all five genes contribute significantly to aphid killing, particularly AprX. This comprehensive host–pathogen transcriptomic analysis provides novel insight into the molecular basis of bacteria-mediated aphid mortality and the potential of PpR24 as an effective biocontrol agent.

INTRODUCTION

The Hemipteran insects, aphids, are highly polyphagous insects characterized by the presence of piercing-sucking mouthparts that enable the acquisition of sap from the phloem of host plants. Around 5000 aphid species are known, feeding on more than 50 plant families (Blackman & Eastop, 1994; Sarwan, 2019). Aphids are one of the most destructive agricultural pests worldwide, responsible for major yield losses in many agro-industrial crops (including wheat, sugar beet, potato, and tobacco), horticultural crops (peppers, spinach, tomato, cucurbits, carrot, lettuce, and legumes) and also in stone fruit trees (Blackman & Eastop, 1994; Sarwan, 2019). Aphids damage crops by direct feeding on the phloem sap, injecting saliva that has phytotoxic effects, and through the transmission of viruses, being a vector for nearly 50% of known insect-borne plant viruses (275 out of 600) (Dedryver et al., 2010). Additionally, the secretion of aphid-produced honeydew onto leaves can promote the growth of sooty moulds, leading to a reduction in host plant photosynthetic capacity (Moir et al., 2018).

Various chemical insecticides, such as thiamethoxam and imidacloprid, are used to control aphid populations in crops (Bahlai et al., 2010; Bass et al., 2014). However, insecticide resistance and the environmental impacts associated with the use of these synthetic chemicals have driven an increased interest in the development of more sustainable, biological approaches for the control of aphid pests. Many natural arthropod predators, such as ladybirds (Coleoptera), green lacewings (Neuroptera), wasps (Hymenoptera), and hoverflies (Diptera), have previously been used to control outbreaks of aphid populations (Kunert & Weisser, 2003; Schmidt et al., 2003). This strategy is usually cost-effective but, with their very short generation time, aphid numbers can very quickly overcome the predator's ability for control, resulting in a runaway infestation. Hence, the use of chemical pesticides can form part of a management strategy for the control of aphid pests, but innovative alternative approaches need to be explored. To address problems raised through the use of conventional and biological pesticides, the use of microbial pesticides is becoming popular in pest management strategies, though most of these focus on Lepidoptera pests like *Plutella xylostella* and *Manduca sexta*. Studies indicate that, besides the more well-known entomopathogenic microorganisms like *Bacillus thuringiensis*, a range of environmental strains isolated from soil and/or plants, such as fluorescent pseudomonads and the nematode-associated bacteria, *Photorhabdus* and *Xenorhabdus*, kill insects (Duchaud et al., 2003; Keel, 2016; Olcott et al., 2010; Waterfield et al., 2001).

Studies over the last 15 years have shown that several plant-associated bacteria, including *Erwinia*, *Dickeya*, *Pantoea*, and *Pseudomonas*, can kill different insect orders through a range of mechanisms including the production of insecticidal toxins or by occlusion of the insect gut causing death by starvation (Costechareyre et al., 2012; Flury et al., 2016; Flury et al., 2019; Stavrinides et al., 2009; Vesga et al., 2020; Vesga et al., 2021). *Pseudomonas* strains exhibit insecticidal activity against agricultural pests including aphids. It is assumed that ingested bacteria can pass through the aphid gut, from the mouth onto the distal end of the foregut, and then to the midgut (Flury et al., 2016; Paliwal et al., 2022; Stavrinides et al., 2009). However, the differential acidity and hydrolytic enzymes within the aphid gut can inhibit or kill ingested microorganisms (Cristofoletti et al., 2003). An initial induction of the insect immune response is triggered upon detection of the pathogen in the gut (Hillyer, 2016). The resulting insect immune response drives the regulation of additional microbial virulence factors to counteract host defences. The first line of host defence, triggered by *E. carotovora*, *P. entomophila*, and *S. marcescens* (Basset et al., 2003; Nehme et al., 2007; Vodovar et al., 2005), includes the production of antimicrobial peptides (AMPs), lysozyme and other digestive enzymes in the gut epithelium (Davis & Engström, 2012). In particular, as part of the lysosomal system, cathepsin-L proteases are predominantly found in the midgut of aphids and other insect species where they function as digestive enzymes for tissue remodelling during insect metamorphosis and various immunological processes (Sapountzis et al., 2014; Wang et al., 2010).

We have previously described a range of bacterial plant isolates that are pathogenic to different species of aphids (Paliwal et al., 2022). One of these, *P. fluorescens* PpR24, was found to colonize different plant species and showed an excellent ability to control aphid infestations. However, the molecular basis of the insecticidal activity of *P. fluorescens* PpR24 was unclear. To address this knowledge gap, we used genome sequencing and RNA sequencing gene expression analysis together with targeted mutagenesis to identify genes with a role in pathogenicity, to provide an understanding of the aphid-killing mechanisms of *P. fluorescens* PpR24. This study provides one of the first detailed studies of a plant-associated bacterium with a Hemipteran aphid pest and some of the key mechanisms used by the bacterium to rapidly kill the aphid.

EXPERIMENTAL PROCEDURES

Draft genome assembly

A list of all bacteria and aphids used in this study is provided in Table S1 and media and growing conditions

are described in Paliwal et al. (2022). In brief, King's medium B (KBM) plates (King et al., 1954) and Lysogeny Broth (LB) (Miller, 1972) were used to grow PpR24 and *Escherichia coli* at 27°C and 37°C, respectively.

Pseudomonas fluorescens PpR24 was sequenced (accession no: NIFJ00000000) at the University of Exeter using the Illumina HiSeq platform (Illumina). The de novo assembly was prepared by the sequencing service through the use of the Velvet assembler tool according to the user's manual (Zerbino, 2010). After assembly, 217 contigs were generated which were further used for functional analysis.

Functional annotation

All FASTA sequences were loaded into Blast2GO (Conesa & Götz, 2008), and BlastX (Johnson et al., 2008) analyses were performed to search *P. fluorescens* PpR24 nucleotide sequences against the nr-protein database using an e-value cut-off of 10^{-3} and reporting a maximum of 20 'hit' sequences per query. Next, mapping was done to retrieve GO terms associated with the hits obtained after a BLAST search. Additional steps in mapping were performed to retrieve UniProt IDs making use of a mapping file from PIR (Non-redundant Reference Protein Database) including PSD, UniProt, SwissProt, TrEMBL, RefSeq, GenPept, and PDB. After mapping, the search results were finally subjected to the function Annotation > Perform Annotation Step menu to perform GO annotation with default parameters.

RNA extraction

Myzus persicae UK insecticide-sensitive aphid clone 4106A was used for the aphid transcript analysis. Aphid samples were snap-frozen in liquid nitrogen and lysed immediately. The total RNA of the control and infected aphids was prepared using the RNeasy Mini kit (Qiagen, UK). To extract total RNA from aphids, the control and bacteria-inoculated aphid sachets (Paliwal et al., 2022) were prepared in four replicates. Four biological bacterial replicate cultures were used to infect aphids in four different sachets each consisting of 10 aphids. After feeding, treated aphids from each bacterial replicate were pooled (4×10 aphids) and homogenized in lysis buffer (700 μL) in a microcentrifuge tube, with a sterilised pestle. Control aphids were pooled (4×10 aphids) from non-inoculated aphid sachets and homogenized in lysis buffer in the same way. To extract RNA from *P. fluorescens* PpR24, a single bacterial colony was inoculated in the Mittler diet at 18°C (Van Emden & Wild, 2020). To avoid bacterial transcript degradation, bacterial culture was suspended in two times the volume of RNA Protect Bacteria Reagent (QIAGEN, Limburg, The Netherlands), according to the manufacturer's instructions. Bacterial cell pellets were harvested by centrifugation at 12,000*g* for 10 min. After centrifugation, the pellet was subjected to either an RNA isolation step or stored for later use at −80°C. All samples were processed for total RNA extraction (RNeasy Mini kit, QIAGEN, Limburg, The Netherlands) followed by DNase I digestion for 15 min (QIAGEN, Limburg, The Netherlands). To ensure complete removal of DNA samples were further processed using an Ambion TURBO DNA-free kit (Invitrogen). Total RNA purity was checked using a NanoDrop (Wilmington, USA) spectrophotometer, and RNA integrity was visualised in a Bioanalyzer 2100 (Agilent Technologies, Santa Clara, USA). RNA samples were visualised on a nuclease-free agarose gel (1%) loaded with RNase-free ×2 RNA loading dye (New England Biolabs, Herts, UK).

Bacteria total RNA enrichment from infected aphids and ribosomal RNA depletion

An improved methodology was employed to enrich the bacterial RNA component from the total RNA of infected aphids, where oligo-dT mix was used to remove >90% of the eukaryotic 18S and 28S ribosomal RNAs (rRNAs), and polyadenylated mRNAs from these mixtures. A maximal amount (25 μg) of total RNA from infected aphids was used as input RNA for enriching bacterial RNA by using MICROBEnrich™ Kit (Life Technologies, Carlsbad, USA), following the manufacturer's protocol. The ethanol precipitation method was used for total RNA purification. The concentration and quality of total RNA obtained were checked as detailed above. The rRNA comprises the major fraction of the transcriptome. To minimise sequencing effort on these abundant molecules, rRNA removal is required before proceeding to cDNA library preparation. Total RNA of aphid (control and treated), control bacteria and enriched bacteria RNA samples were enriched for mRNA by using the Ribo-Zero rRNA removal kit (Illumina, San Diego, USA), following the manufacturer's protocol. The rRNA-depleted RNA quality was assessed by Agilent 2100 Bioanalyzer, through the use of the Agilent RNA6000 Pico Chip according to the manufacturer's instructions. RNA sequencing used for analysis was derived from sequencing done at the Earlham Institute Norwich and submitted to NCBI under Bioproject PRJNA1088857 and accession number SRR28417370-85.

Quantitative PCR analysis

To validate the RNA-Seq analysis data, 10 genes from each aphid and bacteria differentially expressed gene set were selected (Table S2) for confirmation by

quantitative PCR (qPCR). The cDNA synthesis was performed by SuperScript II reverse transcriptase (Invitrogen, UK) with 4 μg of total RNA using random primers as described by the manufacturer (Life Technologies, Carlsbad, USA). For qPCR reactions, 4 μL cDNA at 1/8 dilution was added as a template to SYBR® Green JumpStart™ Taq Ready-mix (Sigma-Aldrich Company Ltd, Dorset, UK) with 500 nM gene-specific primers (Table S3). qPCR was performed on a Corbett Rotor-Gene 6000 machine (QIAGEN, Limburg, The Netherlands) and cycling conditions included 95°C for 10 min (initial denaturation), 40 cycles of 95°C for 15 s (denaturation), 60°C for 15 s (primer annealing step), and 72°C for 15 s (extension). The relative gene expression of the target gene was calculated by applying the formula $2^{-\Delta\Delta CT}$ after normalisation to the control sample (see also Appendix Section A.1).

Gene knockout mutagenesis and complementation

The PpR24 genome analysis identified potential insecticidal toxins that might contribute to aphid killing. Moreover, the RNA-Seq analysis revealed differential expression of these toxin genes. Therefore, selected candidate genes (*tcaA*, *tcaB*, *tcaC*, *rhsA2*, *aprX*, *hypr*) were deleted from the chromosome using an allelic exchange method (Merlin et al., 2002). Up- and down-stream regions of target genes were selected for the design of primers with 'i' (inside) and 'o' (outside) representing the location of primers that are closer to or far from the target gene. Inner primers (Ni and Ci) were comprised of 24-nucleotide-long 5′-tails with complementary sequences and designed to leave the ends of the target gene to maintain the original translation frame in the final construct. Regions of ~500 bp either up- or down-stream of the gene(s) of interest were amplified by PCR with the suitable Ni/No and Ci/Co primers for each selected target using Phusion High-Fidelity DNA Polymerase (Thermo Fisher Scientific, Scotland, and UK). PCR cycling conditions used were as follows: 98°C for 30 s; followed by 30 cycles of 98°C for 10 s, 50°C–70°C (according to primer conditions) for 30 s, 72°C at 30 s kb^{-1}; with a final extension of 72°C for 10 min. PCR products were purified using a Genomic DNA Clean and Concentrator™-25 kit (Zymo Research, Irvine, USA). A NotI restriction site was incorporated into the Ni and Ci primers and BamHI for the No and EcoRI for the Co primers. Except for the *aprX* gene, HindIII for the No primers was used. Due to the presence of complementary sites in Ni and Ci primers, 500 bp PCR products were fused to make a 1 kb product, with the NotI site in the middle, thus 'Splicing by Overlap Extension' (SOE) (Horton et al., 1990). The final 1 kb (SOE) product was then ligated into a pre-digested pK18mob*sacB* cloning vector with fast digest restriction enzymes used for knockout (Thermo Fisher Scientific, Scotland, UK) according to the manufacturer's instructions. Ligations were performed in a 5:1 vector-to-insert ratio using a T4 DNA ligase protocol (Thermo Fisher Scientific, Scotland, UK). The pK18mob*sacB*::SOE linker construct was transformed into electrocompetent DH5α (Invitrogen, Life Technologies, Carlsbad, USA) and plated on Luria Broth (LB) plates (Miller, 1972) containing 50 μg mL^{-1} kanamycin, IPTG and X-gal for blue-white screening. Transformed white colonies were recovered at 37°C and plasmids were isolated from subsequent overnight liquid cultures. To confirm the correct size of the insert, restriction digestion was performed with appropriate enzymes. As pK18mob*sacB*-SOE does not replicate in *Pseudomonas* a triparental filter mating was performed using *E. coli* DH10B (pK18mob*sacB*-SOE) as donor strain, *E. coli* HB101 (pRK2013) as helper strain, and *P. fluorescens* PpR24 as recipient strain. Integration of the plasmid pK18mob*sacB*-SOE into the chromosome of *P. fluorescens* PpR24 by the first crossover was selected on an LB plate supplemented with 50 μg mL^{-1} kanamycin. The second crossover cells were selected by culture on LB plates containing 10% (w/v in water) sucrose. All constructed strains were validated by PCR and DNA sequencing. Complemented strains were generated by cloning the full-length open reading frame gene into the cloning vector pBBR1MCS-2 followed by triparental conjugation into *P. fluorescens* PpR24 and selection on KBM plates supplemented with 50 μg mL^{-1} kanamycin. Complemented strains were verified via PCR as described for the knock-out genes.

RESULTS

Genomic characterization of *P. fluorescens* PpR24

The draft *P. fluorescens* PpR24 genome is 6,176,813 bp in size with a GC content of 60.4%. It includes 46 tRNA genes and 5514 protein-coding genes. Protein-coding genes account for 88% of the total chromosome and have a mean size of 982 bp. Genome comparison of *P. fluorescens* PpR24 against other plant-associated pseudomonads was performed to identify and assess regions of homology. All homologous *P. fluorescens* PpR24 sequences thus identified were matched to the non-redundant InterPro database using BLASTx. The resultant sequences were imported into the Blast2GO Functional Annotation and Genomics (BioBam Bioinformatics, Spain) program which assigned Gene Ontology (GO) terms to 4102 out of 5479 genes. The analysis returned a set of genes, discussed below, that may contribute to virulence against aphids, plant growth promotion, and various aspects of plant colonisation.

Identification of putative insecticidal toxins

The primary functional annotation of *P. fluorescens* PpR24 revealed 10 putative insecticidal toxins in three groups: the Tc toxin complex; the Rhs family; and the secreted metalloproteases (Table 1). The Tc toxin complex genes are co-located in the genome (Figure 1A) and encode four distinct insecticidal toxin complex (Tc) proteins: two TcA-like (TcaA1, TcaB1); one TcB-like (TcaC1); and one TcC-like (TccC2). Such genes are also present in other entomopathogenic enterobacteria including *Photorhabdus luminescens*, *Serratia entomophila*, *Xenorhabdus nematophilus*, and *Yersinia* spp. (Bowen et al., 1998; Waterfield et al., 2001). The Tc toxin locus also encodes two genes for hypothetical proteins (Hypr1 and Hypr2) that appear to be co-transcribed with *tccC2* and may thus contribute to Tc toxin function. InterPro amino acid sequence analysis showed that TcaA1 has a conserved VRP1 (Verprolin) domain, which resembles SpvA, encoded by a plasmid-borne gene in *Salmonella*, which is associated with severe infections in mice (Spink et al., 1994). The only detectable motifs for TcaB1 were two small coil regions. Three conserved SpvB, MidN, and MidC (middle/ N- and C-terminal) domains were found in TcaC1, which shows high similarity to domains present in the corresponding *Ph. luminescens* and *Yersinia pseudotuberculosis* insecticidal toxins (Yang & Waterfield, 2013). The central core of TccC2 has a conserved rearrangement hotspot (Rhs) repeat, similar to that of TccC1 in *Xenorhabdus*. The N-terminal sequence of TccC2 is highly conserved but a high degree of variability was observed at the C-terminal 'toxic' single domain that carries an ADP-ribosyl transferase enzyme motif

TABLE 1 List of putative insecticidal toxin genes in the *Pseudomonas fluorescens* PpR24 genome.

Gene locus	Function	Best hit similarity in NCBI
Class-1 'Tc toxin complex'		
CDH05_22010	Hypothetical protein (Hypr1)	*Pseudomonas* sp. FJ2-5-13 (WP_275622171.1)
CDH05_22015	Hypothetical protein (Hypr2)	*P. fluorescens* (TKK01309.1)
CDH05_22020	Insecticidal toxin complex protein TccC2 (TcC-like)	*P. fluorescens* (TKK01308.1)
CDH05_22025	Insecticidal toxin complex protein TcaC1 (TcB-like)	*P. fluorescens* (MBD8560787.1)
CDH05_22030	Insecticidal toxin complex protein TcaB1 (TcA-like)	*P. fluorescens* (TKK01306.1)
CDH05_22035	Insecticidal toxin complex protein TcaA1 (TcA-like)	*P. fluorescens* (MBD8560789.1)
Class-2 'Rhs family protein'		
CDH05_26805	Rhs family protein	*P. fluorescens* (MBD8560789.1)
CDH05_04585	Rhs-family protein	*P. fluorescens* A506 (AFJ56150.1)
Class-3 'Metalloproteases'		
CDH05_13340	Secreted alkaline metalloproteinase (EC 3.4.24.-), (AprX)	*P. fluorescens* (FH5) ETK39594.1
CDH05_16530	Secreted alkaline metalloproteinase (EC 3.4.24.-), (AprA)	*P. carnis* (WP_198861509.1)

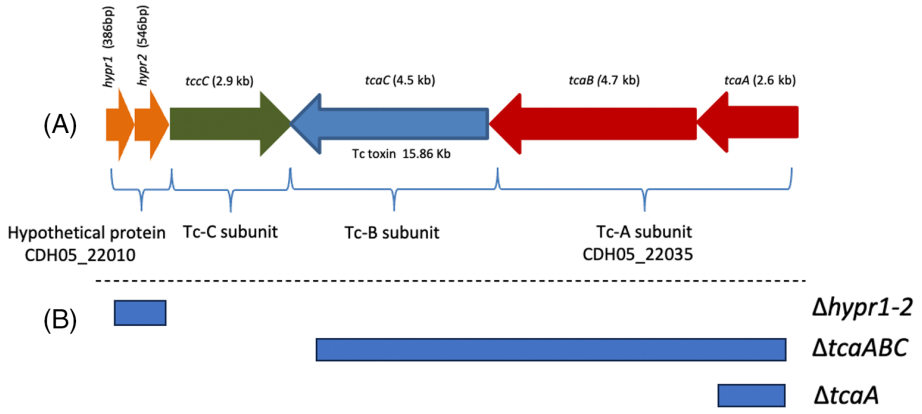

FIGURE 1 Illustration of *Pseudomonas fluorescens* PpR24 toxin complex (tc) mutants. (A) Gene loci consist of three conserved toxin elements (TcA-like, TcB-like, and TcC-like) that are colour-coded (red, yellow, and green, respectively). Representation of deleted gene loci in respective mutants, (B). PpR24 Δ*tcaA* mutant—Deletion of *tcaA* gene region, PpR24 Δ*tcaABC* mutant—Deletion of *tcaA*, *tcaB*, and *tcaC* gene, PpR24 Δ*hypr* mutant—Deletion of *hypr* gene.

(Waterfield et al., 2001). Two putative Rhs toxin genes were also identified (Table 1). These toxins (RhsA1 and RhsA2) contain a YD-peptide repeat with a core/core-extension architecture and carry core extension toxin domains (Jackson et al., 2009; Liu et al., 2009).

Secreted proteins and/or proteases are a further class of biologically active substances that contribute to bacterial pathogenesis toward insects. The PpR24 genome encodes four serine proteases (CDH05_18130, _16555, _16560, and _23010) and two Zn-dependent metalloproteases (AprA and AprX). AprX (CDH05_13340), also named serralysin, and AprA (CDH05_16530), an alkaline protease, are involved in the degradation of AMPs produced by *Drosophila* spp. during the early phase of bacterial infection (Liehl et al., 2006). Both of these metalloproteases were predicted as a third category of toxin in the PpR24 genome. A total of 26 other potential virulence factors observed in the PpR24 genome (including two RTX toxins, two adhesin proteins, an additional three Rhs-family proteins, and three predicted hemolysins/hemagglutinins) are listed in Table S4.

Secretion systems

Secretion systems facilitate the export transport of cargo, often to help with bacterial communication with each other and interactions with potential host organisms. They also promote survival in extracellular environments, enable secretion of virulence factors, and subversion of host defences (Abe, 2009; Chen et al., 2015; Filloux, 2011). Nine macromolecule secretion systems (SS) were identified in PpR24 (two Type I, two Type II, one Type III (T3SS), two Type IV, and two Type VI (T6SS); Table S5). The PpR24 T3SS gene cluster showed maximum similarity with that of *P. fluorescens* KENGFT3 (Town et al., 2016). The main structural genes and corresponding regulator genes (*hrpR*, *hrpL*, and *hrpV*) are all present. Only one gene (CDH05_17280 type III effector *hopPmaJ*) was identified as encoding a putative T3SS effector protein in the PpR24 genome. These are homologous with the *P. syringae* effector HopAS1 and the *P. aeruginosa* effector ExoU, respectively. ExoU is a major *P. aeruginosa* effector and potent cytotoxin with broad substrate activity and phospholipase activity. It plays an integral role in *P. aeruginosa* pathogenicity in *Galleria mellonella* (Miyata et al., 2003), thus marking CDH05_02660 as a potential PpR24 virulence candidate in aphids or other insects. Other secretion systems with potential virulence roles include the two T6SS and their associated 'hemolysin co-regulated protein (Hcp)' (CDH05_19235) and 'VgrG, or Valine-Glycine Repeat Protein G' (CDH05_04595) genes.

Genes for other virulence and niche adaptation traits

Many strains of *P. fluorescens* are known to produce diverse secondary metabolites with antifungal and antibacterial properties (Haas & Keel, 2003; Jousset et al., 2011; Keel, 2016; Raaijmakers et al., 2010). Such metabolites may be important during aphid colonisation, for instance in scavenging key resources from the insect or to grant a competitive edge against resident microbes. The PpR24 genome encodes eight genes similar to those involved in the synthesis of antibiotics such as phenazine and mitomycin (Table S6). In addition, 14 genes encoding proteins involved in pyoverdine biosynthesis and transport were identified indicating an intact pyoverdine-dependent iron-uptake system. We also identified 19 PpR24 genes with predicted roles in reactive oxygen species (ROS) scavenging: two superoxide dismutases; six catalases; and 11 peroxidases (one cytochrome C peroxidases, three glutathione peroxidases, four DyP-type peroxidases, two thiol peroxidases, and four alkyl hydroperoxidases; Table S7). Such genes are found in many pseudomonads (Choi et al., 2007; Kang et al., 2007). Homologues of putative ROS regulators were also discovered, such as the MarR-family redox-stress sensors, PqrR and OhrR, and the LysR-like regulator OxyR; these three regulators share close sequence similarity with the corresponding *P. aeruginosa* regulators (Cornelis et al., 2011). The presence of these oxidative stress resistance genes indicates a robust capacity to respond to and resist, environmental and host exposure to redox stress.

Plant-associated bacteria are well known for mediating positive interactions with, and efficiently colonizing, plants using mechanisms including chemotaxis and motility (Alsohim et al., 2014; Kamilova et al., 2005). We identified a set of Che system genes (*cheA*, *cheB*, *cheR*, *cheW*, *cheY*, and *cheZ*) responsible for signal transduction and chemotaxis (Table S8). In addition, 25 methyl-accepting chemotaxis protein (*mcp*) genes were found, indicating that PpR24 likely senses and responds to a wide range of environmental and intracellular chemotactic signals (Table S8). Forty-two flagellar gene machinery complex genes were found, including those encoding biosynthesis, regulation, structure, and motor functions (Table S9).

Simultaneous transcriptional profiling of aphids and bacteria to identify potential pathogenicity factors and targets

Although the genome sequence analysis allows the identification of a range of putative virulence factors, we sought to gain insight into which genes are expressed by the bacterium during infection of the aphid. To do this, gene expression patterns during the aphid

infection process were investigated using an RNA-Seq approach. This involved the isolation of total RNA from infected aphids as well as non-infected aphids and the PpR24 pre-infection inoculum. Bacterial and aphid transcripts from infected samples were separated in silico. A systematic approach to optimize the experiment was carried out using our aphid-feeding system and a range of bacterial inoculum densities and sampling times (see Appendix Section A.1.1 and Table S10). We found that using a bacterial inoculum of 10^7 CFU mL^{-1} in the feeding sachets and sampling aphids 38 h after addition to feeding sachets provided sufficient depth of sequence coverage for bacterial transcripts ($\sim 7.5 \times 10^5$ reads per transcript) to enable differential gene expression effects to be determined (Table S10).

A total of 193 aphid genes (1% of the total, 0.6% up- and 0.4% down-regulated) and 1325 PpR24 genes (24% of the total, 542 up- and 783 down-regulated), were differentially regulated at 38 h post-infection (fold-change >2.0; $p < 0.05$; Figure 2A,B). Of the 542 upregulated and 783 down-regulated PpR24 genes, 121 genes showed a fold increase of >5, and 155 genes were downregulated by >5 fold.

To provide additional confidence in the outcomes of the RNA-Seq analysis, 20 differentially expressed aphid/bacterial genes (10 of each) were selected for expression analysis by qPCR (Table S2) based on major alteration (and low replicate variation) in relative levels during infection (as determined by RNA-Seq). The 20 genes showed concomitant expression changes by RNA-Seq and qRT-PCR (Table S2) with a comparative Pearson coefficient R^2 value of 0.99, thus indicating that the differential expression revealed by RNA-Seq is valid and robust.

Transcriptional profile of *P. fluorescens PpR24* after aphid infection

Upregulation of *P. fluorescens* PpR24 iron-acquisition systems

Genes encoding the biosynthesis and uptake of siderophores were notably upregulated. This includes 15 genes required for pyoverdine biosynthesis and utilisation, with an average induction of 12.1-fold. *pvdS* displayed the greatest induction (47.5-fold) (Table S11A, Figure 3). In addition, 11 other genes predicted to be involved in ferri-siderophore or ferric-iron uptake were also induced in the aphid by an average of 11.6-fold (Table S11A) along with other genes known to be activated by iron restriction (*sodA* and *bfd*, induced by 10.1- and 15.4-fold, respectively; Table S11A). Eight haem-acquisition, utilization, and regulation genes were also upregulated, by an average of 16.2-fold, with the gene encoding haem oxygenase (required for release of iron from haem) showing the greatest induction (58-fold; Table S11A). Genes specifying the Efe ferrous-iron uptake system (Kammler et al., 1993) were upregulated by more than 15-fold (Table S11A) and those encoding uptake of the divalent metals Mg^{2+} and Zn^{2+} were also increased (by 2.6- to 4.1-fold). These findings indicate that PpR24 is exposed to an environment that is iron-restricted (and potentially limited for other metals also) upon aphid infection which results in a de-repression of the iron-uptake machinery, likely dependent on the iron regulator Fur. Moreover, functional enrichment analysis showed genes associated with iron uptake (phosphopantetheine, vitamin, and amide) and binding (phosphopantetheine, vitamin,

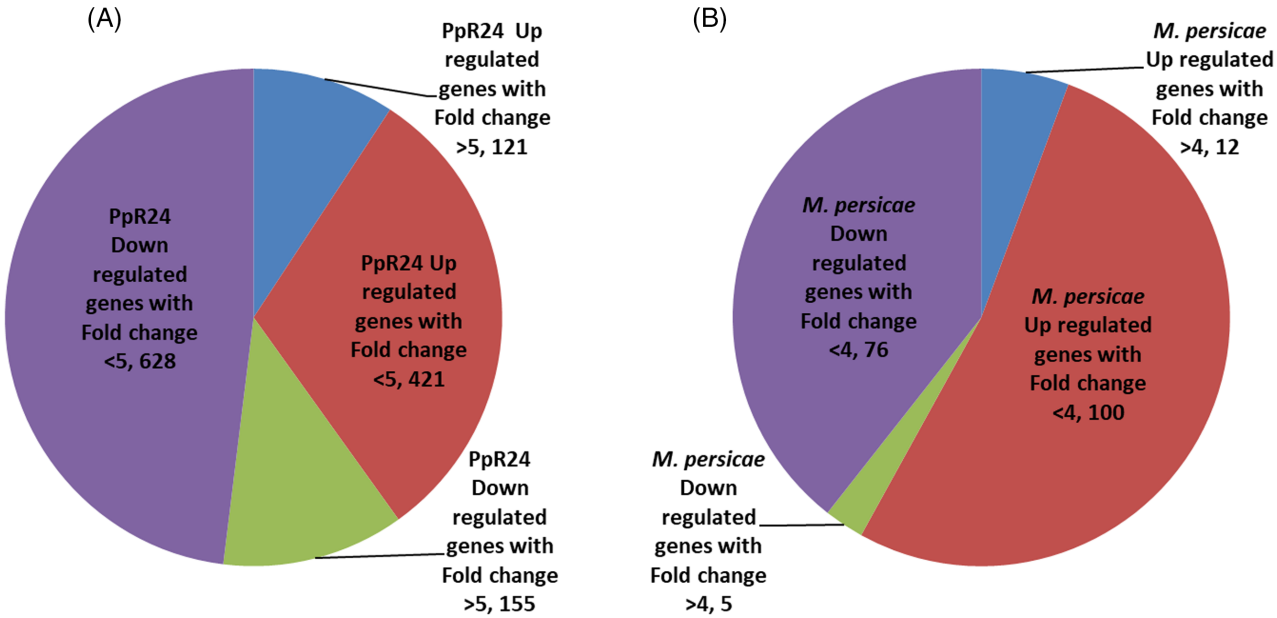

FIGURE 2 Differentially expressed genes (DEGs) in *Pseudomonas fluorescens* PpR24 (A) and *Myzus persicae* 4106A (B) after 38 h of infection. The pie charts display the number of DEGs exhibiting changes that are more and <4-fold change.

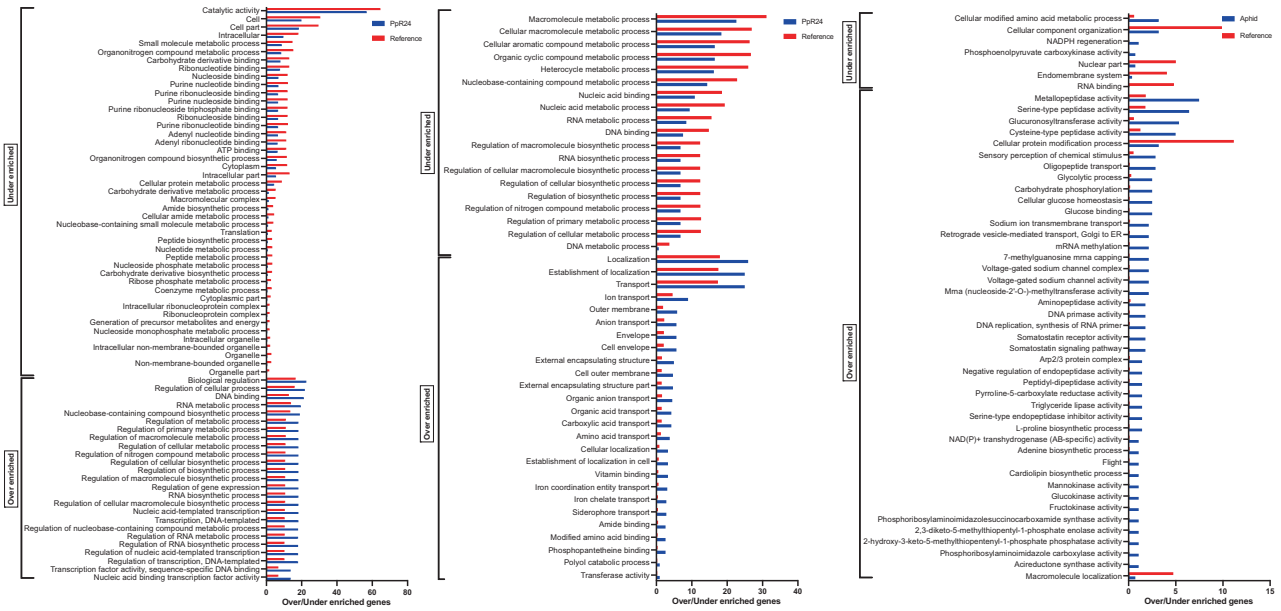

FIGURE 3 GO term enrichment analysis on transcriptomic data in *Myzus persicae* 4106A (A). *Pseudomonas fluorescens* PpR24 (B,C). The figure represents all the significant GO-term categories found significantly enriched compared with the reference set (all genes present in the RNA-Seq data) after a Fisher's exact test and Benjamini and Hochberg multiple testing correction (FDR, 0.025—*Myzus persicae* 4106A (A) and FDR, 0.05 *Pseudomonas fluorescens* PpR24 (down-regulated) (B) and up-regulated (C)). The test set percentage indicates the percentage of differentially expressed genes belonging to a GO term category compared with all differentially expressed genes used in the GO-term analysis while the reference set percentage indicates the percentage of a particular GO-term category compared with all genes with GO-terms in the RNA-Seq data.

and amide) were over-enriched with 2%–4.5% upregulated gene sets.

Virulence factors, toxins, and oxidative stress

The expression of putative virulence factors such as the T4SS and extracellular alkaline metalloprotease (*aprX*) was increased by 3- to 5-fold, whereas downregulation (2- to 4-fold) of other genes associated with insect pathogenicity was seen, for example, the *tcaC* subunit of Tc toxin and Rhs family proteins (Table S11B). The upregulation of genes encoding antioxidant proteins (glutathione S-transferase, manganese superoxide dismutase, rubredoxin, glutaredoxin, thioredoxin, and thiol peroxidase Tpx-type) indicates exposure to aphid oxidative stress defence mechanisms (Table S11B), although three catalase genes and the alkyl hydroperoxide reductase F subunit gene were 2.2- to 8.9-fold down-regulated, which contrasts with this view (Table S11B).

Flagella and adhesion genes

The downregulation by 3- to 10-fold of 26 genes associated with adhesion (pili and fimbriae) systems and their assembly was observed suggesting the bacteria were not in a biofilm-forming behaviour at the time of infection. In addition, five methyl-accepting chemotactic genes were upregulated and two were downregulated by 2- to 2.5-fold (Table S11C). The elevated level of a few flagellar biosynthesis genes (*flgB*, *flgC*, *flgE*, and *flaB*), together with the upregulation of two pili assembly proteins by 2-fold, was also observed suggesting that motility was activated during this phase of the infection process (Table S11C).

Iron rationing response

The downregulation of various genes associated with sulphur assimilation (taurine, alkanosulphonates), the respiratory chain (cytochrome oxidase), iron storage (two bacterioferritins, 4.5- and 6.5-fold repressed) and oxidative stress (three catalases, alkyl hydroperoxide reductase, the iron-dependent superoxide dismutase; 2.2- to 8.8-fold repressed) was observed (Table S11B and D). Such genes are known to be suppressed under iron restriction as part of an iron rationing response (Amich et al., 2013; Kawakami et al., 2009), and so this regulatory response correlates well with the induction of iron transporters reported above.

Impact of infection by *P. fluorescens* PpR24 on the aphid transcriptional profile

Analysis of the aphid transcriptome showed just 193 differentially regulated genes (112 and 81 were up- and

down-regulated, respectively). This difference in the degree of regulatory adjustment likely reflects the inclusion of all tissues within the aphid RNA extractions; different tissues/organs would be expected to respond to PpR24 infection distinctly depending on tissue type and degree of PpR24 exposure, and such effects would obscure differential expression effects. The highest degree of upregulation was 15.4-fold (uncharacterized LOC100570877; a gene of unknown function) and indeed most (100 out of 112 genes) upregulation was modest (within the 2- to 4-fold range). Of the 81 genes that were downregulated, the greatest degree of repression was 39.2-fold (carotenoid desaturase) with only five genes reduced by >4-fold and the remainder decreased by 2- to 4-fold (Table S12). Thus, the overall degree of differential expression observed was low.

Differential expression of immune and gut-specific defence genes

During infection of the aphid by PpR24, a 2- to 3-fold-upregulation of genes encoding two cuticular-like proteins, a chemoreceptor protein ('takeout'), and three proteins with innate immune motifs (sterile alpha and TIR motif, leucine-rich repeat and Pv-fam-d protein) was observed (Table S12A). Genes involved in the cellular uptake of xenobiotics (transporters—nose resistant to fluoxetine transporter of saliva and transporter–trehalose) were increased by 2-fold (Bansal et al., 2014). The gene encoding the major antioxidant enzyme of saliva, 'gamma-glutamyltranspeptidase 1-like', was reduced (by 15-fold) along with genes (by 3- to 4-fold) encoding xenobiotic metabolism proteins (such as UDP-glucuronosyltransferase, esterases, and cytochrome b561-like) (Table S12A).

Four protease-related genes showed higher expression (3.55- to 2.32-fold) and four showed reduced expression (3.55- to 2.04-fold) in treated aphid profiles compared with controls (Table S12A). Higher expression levels of all putative cysteine proteases, cathepsin B-N, and 'TPA_inf: cathepsin B' were reported in treated aphids (Rispe et al., 2007). The serine protease (venom protease) and matrix metalloproteases are involved in defence mechanisms (Kutsukake et al., 2004). The transcript levels for these genes exhibited an increase in treated aphids ranging from 2- to 3-fold (Table S12B). The putative protease genes with lower transcript levels in treated aphids included four genes encoding predicted cathepsins (cathepsin B and B-like) and the aminopeptidase N-like protein, with reductions in expression of 2- to 2.8-fold and 3.5-fold, respectively (Bansal et al., 2014) (Table S12B). Two genes encoding serine protease inhibitors (regucalcin-like isoform and angiotensin-converting enzyme-like isoform X3) were upregulated 2.2- and 4-fold, respectively (Bansal et al., 2014) (Table S12B). Functional enrichment analysis of *M. persicae* differentially expressed genes (at FDR 0.025) showed sensory perception, proteolysis, and glucuronosyltransferase activity were majorly enriched with more than 2.5% of differentially expressed genes (Figure 3).

Differential expression of cell locomotion, cytoskeleton, and other cellular process

The myofibrillar gene '*titin*' involved in flight and muscle contraction increased in expression by 2.28-fold along with expression of muscle contractile regulator 'PDZ and LIM domain Zasp isoform X12' (2-fold) (Lin et al., 2014) (Table S12C). Elevated levels (2.44-fold) of the major chaperone protein 'Tubulin-specific chaperone cofactor E', which is involved in the normal growth and functioning of neuromuscular synapses, were observed (Table S12C). The nesprin gene, associated with the nerve cell cytoskeleton, was also induced (2.4-fold) (Morel et al., 2014). The kintoun gene, which is needed for the pre-assembly of axonemal dyneins, was repressed 2.1-fold (Von Morgen et al., 2015) (Table S12C). Two defence signal molecules Hdd11 and craniofacial development 2-like partial, which are required for nervous development and cell proliferation, were downregulated by 2- and 3-fold, respectively. The gene associated with the adrenergic receptor signalling pathway '*arrestin domain-containing protein 3*' was also decreased by 2.5-fold (Puca & Brou, 2014) (Table S12C).

Mutagenesis of candidate virulence factors

To determine whether the putative virulence genes described above are involved in the PpR24 infection of aphids, a gene mutagenesis approach was employed. The genomic analysis identified six genes (*tcaA*, *tcaB*, *tcaC*, *rhsA2*, *aprX*, and *hypr*; Figure 1) with potential roles in virulence based on induction in the aphid and/or their predicted toxin function. These genes were thus deleted from the chromosome using the allelic exchange method (Merlin et al., 2002) resulting in the production of six mutants: three single genes Δ*tcaA*, Δ*rhsA2*, and Δ*aprX*, and three combinations of genes, Δ*tcaArhsA2* (Δ*tcaA*, Δ*rhsA2*) Δ*tcaABCrhsA2* (Δ*tcaABC*, Δ*rhsA2*) and Δ*hypr* (Δ*hypr1-2*). The absence of the corresponding toxin gene(s) was confirmed by PCR using primers (Table S2) flanking the targeted region.

The three single-toxin-gene mutations (Δ*tcaA*, Δ*rhsA2*, and Δ*aprX*) caused a partial attenuation of PpR24 pathogenicity in the aphid, with a 30–40% reduction in aphid death for Δ*tcaA* and Δ*rhsA2*. The greatest decrease in aphid mortality was observed for the Δ*aprX* (metalloprotease) mutant which showed an 80% reduction in mortality, with just 20% aphid mortality at 48 h (100% aphid toxicity with the mutant was only observed after 80 h; Figure 4). However, since all

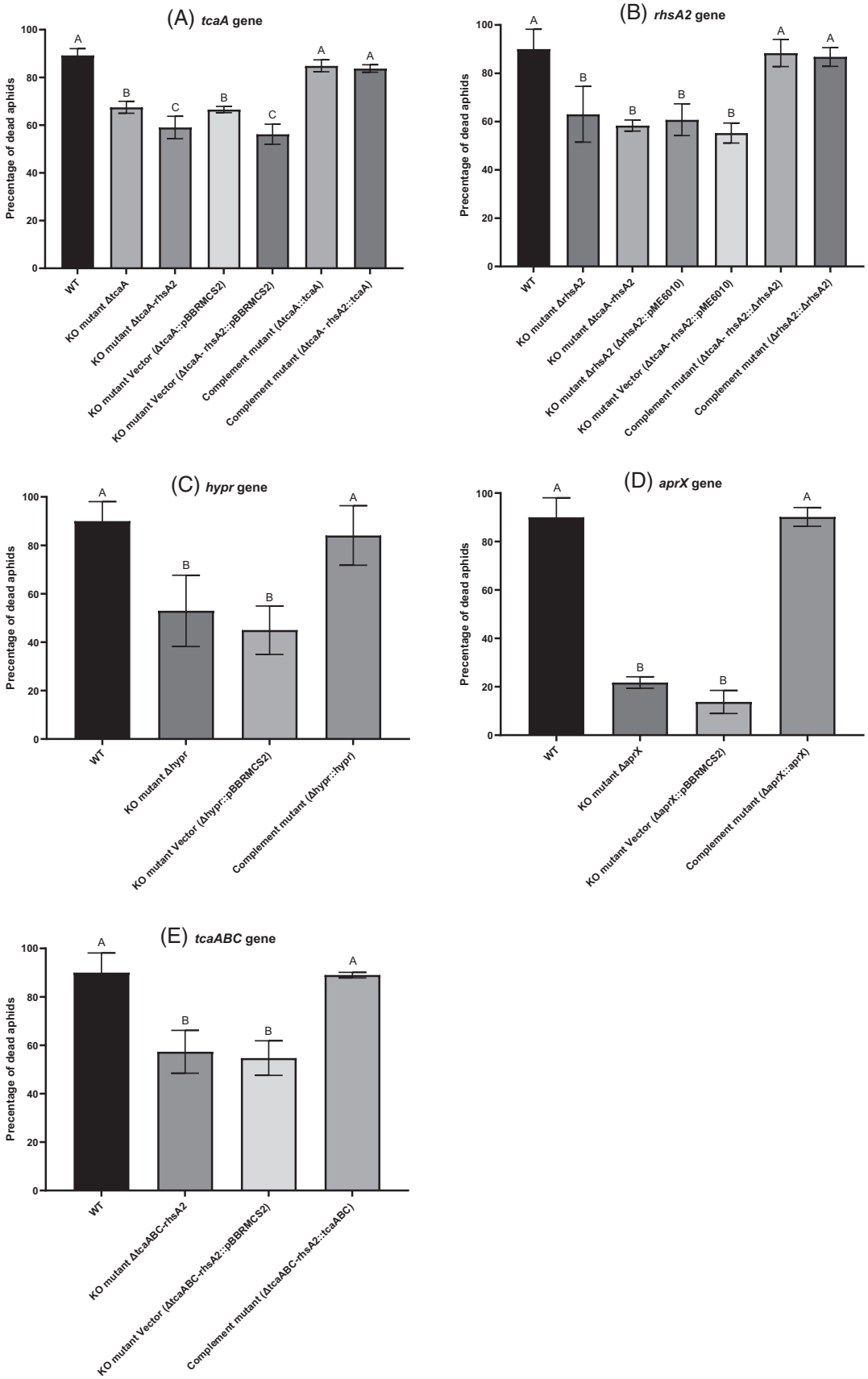

FIGURE 4 Legend on next page.

three mutants showed only a partial loss of aphid killing it is likely that the virulence phenotype of PpR24 is multifactorial. To test for additive effects of toxin gene mutation on virulence, double and multiple mutants were constructed and tested for virulence. Attempts were made to generate all possible double or multiple mutant combinations but only one double toxin mutant *ΔtcaA-rhsA2* (deletion of *tcaA* gene and *rhsA2* gene) and multiple mutant *ΔtcaABC-rhsA2* (deletion of Tc–AB subunits genes [*tcaA*, *tcaB*, and *tcaC* gene] and *ΔrhsA2*) could be generated (Figure 1). These mutants displayed a reduction from 90% to 56% in aphid mortality (Figure 4), which is not significantly different from the effects of the corresponding single deletions.

To confirm the association of the toxin gene deletions with the observed reductions in virulence, the corresponding toxin-gene mutants were cloned into the broad host range vector pBBRMCS1-2 (except *rhsA2*, which could not be cloned into this vector and was thus cloned in pME6010) to complement the mutation(s). The resulting plasmids (and vector only as controls) were transformed into the relevant mutant strain to enable complementation and test the effect on aphid mortality. All complemented strains restored aphid death to levels similar to that of the wild-type PpR24. The vector controls gave levels of mortality similar to those of the non-transformed mutants. There were no significant differences between the wild type and the complemented strains; the same was seen in the comparison between all the mutants with their respective vector controls (Figure 4). The results thus indicate that the observed restoration of virulence in the complemented strains was due to the reversal of the mutant phenotype by the complementing toxin gene and that the observed virulence phenotypes are thus associated with the toxin and protease genes present in the chromosome.

DISCUSSION

In this work, we have sought to gain insight into the mechanisms employed by *P. fluorescens* PpR24 to kill aphid pests, a largely understudied area. Our previous work (Paliwal et al., 2022) showed PpR24 to be particularly effective in the killing of six aphid species. However, in similar toxicity assays variations in aphid killing efficacy were demonstrated indicating significant variations in both aphid susceptibility and bacterial pathogenicity. Further investigation at the molecular level was therefore pursued to enhance our understanding of this *Pseudomonas*–Hemiptera interaction.

We considered our observations in the context of both insect killing as well as for the control of non-insect targets to gain an understanding of PpR24 relative to other insect-killing *Pseudomonas* strains (i.e., does it show novelty or not because it targets a Hemipteran insect). PpR24 virulence mechanisms against aphids are consistent with earlier findings of *P. entomophila* pathogenesis inside Diptera insects like Drosophila. The PpR24 genome was found to contain one toxin complex (Tc), two Rhs family toxins, two alkaline proteases (*aprX*, *aprA*), hemolysins (exotoxins), and cell surface–associated virulence factors (hemagglutinin-like adhesins), several of which are implicated in toxicity to insects. However, it did not encode a homologue of the Fit (mcf) toxin often found in *P. protegens* and *P. chlororaphis* (Ruffner et al., 2015). An array of commonly identified gene systems (including chemotaxis, motility, and adhesion factors) associated with and facilitating the colonisation of a large range of habitats (which may include insects) were also identified in PpR24. PpR24 lacks the secondary metabolite genes that encode the production of polyketides, pyoluteorin and 2,4-diacetylphloroglucinol (DAPG), pyrrolnitrin, and hydrogen cyanide which are antimicrobial compounds often associated with *P. fluorescens* species-complex strains for the suppression of soil-borne plant pathogenic fungi and oomycetes (Gallagher & Manoil, 2001; Garrido-Sanz et al., 2023; Haas & Défago, 2005) and also implicated in *Caenorhabditis elegans* killing by *P. aeruginosa*. Several of these metabolites have been reported in other plant-beneficial pseudomonads, such as *P. putida* strain 1A00316, which has insect pathogenicity (Flury et al., 2016; Guo et al., 2016). The coordinated regulation of DAPG and pyoluteorin serves as a strategic approach for *P. protegens*, enabling the efficient deployment of secondary metabolites with distinct functions in both cooperative and competitive microbial interactions (Yan et al., 2017). Notably, none of these factors is universally shared by all these strains or are exclusive to insecticidal strains (Lugtenberg & Kamilova, 2009; Mercado-Blanco & Bakker, 2007), but their absence may reflect a potential niche-specialization process toward insects and away from soil or rhizosphere habitation.

FIGURE 4 (A–E) Assessment of aphid mortality by *Pseudomonas fluorescens* PpR24 mutants and complemented mutants. Mortality assay showing the percentage of dead aphids ($N = 10$) at 48 h after ingestion of artificial diet inoculated with the indicated bacterial strains (10^7 CFU mL^{-1}). Error bars represent the standard error of the mean of three biological replicates. ANOVA detected statistically significant differences ($p < 0.05$) and significant differences determined by Tukey–Kramer HSD are indicated by letters (where different letters indicate statistically significant differences). Key—PpR24 wildtype (WT), Deletion mutant (Δ gene), Complement mutant (Δ gene::gene), and Deletion mutant vector (Δ gene::vector). Mutated genes—Δ*tcaA* (deletion of *tcaA*), Δ*tcaABC* (deletion of *tcaA*, *tcaB*, and *tcaC* genes), Δ*rhsA2* (deletion of *rhsA2* gene), Δ*tcaABC-rhsA2* (deletion of *tcaA*, *tcaB*, and *tcaC* and *rhsA2)* Δ*hypr* (deletion of hypothetical protein genes 1 and 2) and *aprX* (deletion of metalloprotease *aprX* gene).

Although the genome sequence analysis provided some clues into potential mechanisms of aphid killing, we sought a more definitive insight. We therefore employed simultaneous analysis of the transcriptional response of the host (aphid) and the pathogen (PpR24) during infection at a single time point where sufficient bacterial reads could be recovered. Although this does not provide a complete picture of the expression activity during the entire process of infection, it still affords a valuable understanding of the late stage of infection. Iron is essential for most bacteria, however both animals and plants have evolved elaborate immune strategies ('nutritional immunity') to limit the availability of iron to pathogenic bacteria (De Gregorio et al., 2001; Irving et al., 2001; Nappi & Vass, 2000). Bacteria cope with iron deprivation through the induction of iron transporters and by iron rationing (Cornelissen, 2003; Noinaj et al., 2012). During aphid infection, PpR24 upregulated systems for ferric-iron acquisition (such as pyoverdine-mediated iron uptake), haem-acquisition, and other known/potential iron-transport systems, which indicates a regulatory response to counter iron-limiting conditions experienced within the aphid (Lim et al., 2012). Pyoverdine has been shown to play a role antagonism and biocontrol efficacy of *P. fluorescens* Pf275 against a fungal pathogen (Dutta et al., 2020) which suggests that its upregulation in the aphid may contribute to aphid killing.

Bacterial iron regulation is linked to managing oxidative stress due to the role of iron in generating harmful reactive oxygen species (ROS). Excess iron is stored safely within cytosolic iron-storage proteins like bacterioferritin or ferritin, stored as inert iron cores inside protein shells (Huang et al., 2002; Ma et al., 1999). Previous studies (e.g., in *P. syringae*) have shown that under low-iron conditions, the expression of *bfr* (bacterioferritin) is reduced, and the *bfd* gene (bacterioferritin-associated ferredoxin) is upregulated (Bronstein et al., 2008; Ochsner et al., 2000; Palma et al., 2003; Yao et al., 2011). This study observed similar patterns in PpR24 colonizing aphids, with downregulation of *bfr* genes and upregulation of *bfd*, indicating a response to low iron levels and the utilization of intracellular iron stores (Table S11A). PpR24 exhibits an iron-rationing response in aphids, as seen in the differential regulation of superoxide dismutase (Sod) genes, *sodA*, and *sodB*. SodB utilises iron as a cofactor and expression of the corresponding *sodB* gene was downregulated (2.3-fold), presumably as part of the iron-rationing response (Hassett et al., 1997; Polack et al., 1996). In contrast, the gene encoding SodA (employing manganese as a cofactor) was induced, probably to compensate for the reduced *sodB* expression in response to low iron levels. These changes are in line with the reduced expression of iron-dependent enzymes under iron-limited conditions and thus further indicate that PpR24 is exposed to an iron-restricted environment during aphid infection (Touati, 2000). *P. fluorescens* Pf-5 has two SODs and six catalases (Paulsen et al., 2005).

Our transcriptome analysis also identified differentially expressed aphid genes. Some interesting observations were made that are useful for understanding how the aphid responds to infection by PpR24. The feeding of the aphids on food sachets containing PpR24 led to the induction of only a few aphid saliva- and gut-specific defence mechanisms. This included induction of the aphid saliva 'takeout' gene and genes encoding other gut digestive enzymes (glucosidase and lipases); this might suggest a role in actively degrading bacterial cell components. It is possible that the induction of proteases (such as the cathepsins, aminopeptidase N-like and venom protease, digest bacteria) in the aphid upon PpR24 infection represents a bacterial killing mechanism. It has been shown that the major gut-specific genes, glucosidase, aminopeptidase N-like protein, facilitated trehalose transporter, and solute carrier family 46 member 3-like, are expressed during feeding (Cristofoletti et al., 2006; Ye et al., 2014). This suggests a link between major facilitator super domain and solute carrier family transporter expression and the homeostatic control of absorption of amino acids, sugar, and lipids from the midgut. These results indicate that following ingestion of PpR24, the aphid employs a suite of saliva and midgut defensive countermeasures against bacterial pathogenicity.

The infected aphids responded to bacterial infection through activation of an 'uncharacterized family 31 glucosidase KIAA1161-like' gene with predicted glucosidase activity that may play a role in bacterial recognition. Up-regulation of stress-related genes such as 'cuticular', 'takeout', leucine-rich repeat domain, and 'sterile alpha and TIR motif-related' (SARM), in response to infection, is consistent with an insect response to stress (Hou et al., 2013; Marmaras et al., 1993; Pal et al., 2008; Waterhouse et al., 2010). However, the absence of any immune gene expression, and the downregulation of drug metabolism genes and lysozyme indicate that the *M. persicae* defence responses are not fully activated which would be expected to facilitate PpR24 colonisation of the aphid host. As compared with other Hemiptera, this relatively limited response to PpR24 infection highlights the restricted number of antimicrobial defence mechanisms reported in aphids relative to other insects (Gerardo et al., 2010). It is important to frame these observations in the context of the infection, just a few hours before the aphids start to die. Thus, the relatively low number of differential gene changes may reflect this late stage and it will be important to develop an optimized method for examining gene expression changes at earlier time points to fully understand bacterial and aphid responses.

Given the observations made, we questioned what the likely mode of infection might be. For example, it could be that the T3SS facilitates the entry of PpR24

into aphid cells, as described for *P. aeruginosa* PA14 in a *Galleria mellonella* caterpillar model (Miyata et al., 2003). The T3SS of *Ph. luminescens* TT01 is likewise involved in insect host cell invasion and mediates effector protein injection into host cells in the early stage of infection. Entry of these effector proteins modulates the host endocytic system, which leads to the internalisation of bacteria (Brugirard-Ricaud et al., 2005). A type III secretion system (T3SS) gene cluster related to the *hrc*/*hrp* T3SS of the plant pathogen *P. syringae* was identified, with seven putative effectors identified. Type III secretion systems have also been found in strains of *P. fluorescens* (Preston et al., 2001). Paulsen et al. (2005) found no T3SS in the genome of *P. fluorescens* Pf-5 which has biocontrol potential against soilborne plant pathogens. Only one T3SS was observed in the PpR24 genome, unlike some plant pathogenic and insect-associated bacterial strains, that harbour two gene clusters, for example, *P. stewartia*, which alternates between its insect vector and the plant host. The *P. stewartii* Hrp-Hrc T3SS is essential for maize pathogenesis, but a second T3SS (*Pantoea* secretion island 2 [PSI-2]) of the Inv-Mxi-Spa T3SS family, is also present. This is typically found in animal pathogens and is required for *P. stewartii* persistence in its flea beetle vector, *Chaetocnema pulicaria* (Melsh) (Correa et al., 2012). Another pathogen, *Yersinia enterocolitica*, uses its T3SS intracellularly in cells to enable bacterial replication (Walker et al., 2013). Our study showed that some T3SS genes were downregulated indicating they were unlikely to be used at the 38 h stage of infection, so a more detailed time course of the infection process will be required to determine whether the T3SS is important, combined with investigation of corresponding T3SS mutants. A different secretion system, T6SS, enabled invasion by *P. protegens* of the Lepidopteran *Pieris brassicae* and was observed to cause substantial modifications to the insect gut microbiome, influencing Enterobacteriaceae, a predominant group of commensal gut bacteria (Vacheron et al., 2019). Whether this mechanism could be employed by PpR24 with one of its two T6SS has yet to be investigated.

The PpR24 transcriptomic data revealed the expression of many genes involved in defence and stress responses, which are likely employed to counteract the insect response. We observed higher expression of the *aprX* protease gene compared with other protease and toxin genes such as *aprA* and *tcaC*. Notably, some of the toxin genes identified in the genome were not upregulated at 38 h yet clearly played a role in aphid killing, as observed for the deletion mutants, thus suggesting expression of the genes at an earlier time point. The induction of protease genes (*aprA* and *aprX)* upon aphid infection may enable the degradation of cells and tissues to facilitate colonisation of sites within the insect beyond the gut lumen. Besides protein factors, many entomopathogens produce toxic secondary metabolites that impair host machinery or compete with beneficial microbes (Duchaud et al., 2003; Vodovar et al., 2006). The YD repeat/RHS element found in the 'yo**u** **c**annot **p**ass' (Ucp) protein of *Pantoea stewartii* enables this bacterium to colonise the gut of the pea aphid and form aggregates, leading to reduced honeydew excretion and host death (Stavrinides et al., 2010). Similarly, our findings show that the expression of the related *rhs*-like gene of PpR24 inside the aphid gut promoted host death. *P. entomophila* secretes proteases, like AprX, that cause hemolymph bleeding and anaphylactic responses during invasion in Drosophila and silkworms (Liehl et al., 2006). The *aprX* gene deletion resulted in a considerable decline in aphid death (by 80%), which suggests that this extracellular protease assists pathogen colonisation possibly by direct damage to host tissue and/or by interference with the immune response. A previous study showed a role for two *P. aeruginosa* proteases, alkaline protease (AprA) and the elastase (LasB), in the degradation of exogenous flagellin and prevention of flagellin-mediated immune recognition inside the insect host (Casilag et al., 2015). *P. putida* strain 1A00316 has diverse nematocidal factors including protein-alkaline metalloprotease AprA (Guo et al., 2016). AprA from the insect pathogen *P. entomophila* has been identified as a contributor to virulence against *Drosophila melanogaster*, potentially protecting the bacteria against the insect immune response (Liehl et al., 2006). AprA has also been reported in *P. fluorescens* Pf-5 (Loper et al., 2016) and *P. protegens* CHA0, respectively (Flury et al., 2017). Thus, the AprA protease of *P. fluorescens* PpR24 (and AprX) may play a similar role in subverting aphid immune responses.

To further explore the role of factors suspected to promote PpR24 killing of the aphid, we employed a reverse genetics approach to target five genes encoding putative toxins that were induced upon aphid infection. Our findings showed that *tcaA*, *rhsA2*, and *hypr* KO mutants all exhibited a significantly lower killing activity toward *M. persicae* than the wild type. However, respective aphid mortality for each of these three mutants remained relatively high at 68%, 62%, and 50%, respectively, indicating all contribute to, but none are essential for, aphid death. These genes may be components of the same killing mechanism (e.g., proximity of *hypr* to *tcaA* suggests that they are part of the same toxin system). Two multiple mutants (Δ*tcaA*-Δ*rhsA2* and Δ*tcaABC*-Δ*rhsA2*) were also constructed and both showed slight further reductions in aphid mortality from 62%–68% to 59% and 57%, respectively. However, these reductions were not significant in comparison with the corresponding single mutants. In *Salmonella*, the VRP1 domain of the SpvA protein (similar to the Tc-A subunit encoded by *tcaA*) and ADP-ribosyltransferase domain of SpvB toxin

protein (equivalent to the Tc-B subunit encoded by *tcaC*) are involved in depolymerization of actin, destruction of the cytoskeleton and cytotoxicity (Boyd & Hartl, 1998; Gotoh et al., 2003). In the current study, the reduction of aphid mortality to 68% and 52% in the Δ*tcaA* and Δ*tcaABC* mutants, respectively, is consistent with similar roles for the VRP1 domain of the TcaA protein and the SpvB domain of TcaC protein in actin condensation leading to cell dysfunctions in the aphid gut including increased cell membrane permeability and disruption of cell junction rearrangements.

In summary, the genome sequence analysis combined with comprehensive transcriptome profiling of bacteria and aphids together has provided a novel insight into the responses of both the aphid and PpR24 during the infection process. We have identified several key genes that enable PpR24 to kill aphids and our analysis suggests there may be regulated expression of virulence factors during different periods of the infection. This is one of the first studies to examine how a *Pseudomonas* bacterium kills a Hemipteran insect pest and lays the foundation for further detailed analysis to develop methods that examine the timing of gene expression at different infection stages and to unravel the host targets and niche of expression. Importantly, these observations confirm that PpR24 plays an active role in killing the aphid after oral ingestion, thus the bacterium could have potential use as an effective biocontrol agent.

AUTHOR CONTRIBUTIONS

Mojgan Rabiey: Data curation; formal analysis; validation; writing – review and editing; visualization. **Deepa Paliwal:** Methodology; data curation; validation; visualization; writing – original draft; writing – review and editing; investigation. **Timothy H. Mauchline:** Supervision; writing – review and editing; validation. **Keywan Hassani-Pak:** Supervision; validation; writing – review and editing. **Ralf Nauen:** Supervision; validation; writing – review and editing. **Carol Wagstaff:** Supervision; validation; writing – review and editing. **Simon Andrews:** Supervision; validation; writing – review and editing. **Chris Bass:** Supervision; validation; writing – review and editing. **Robert Jackson:** Supervision; validation; conceptualization; methodology; investigation; funding acquisition; visualization; project administration; writing – review and editing; resources.

ACKNOWLEDGEMENTS

We thank Primitivo Caballero, Jesus Murillo, and Leopoldo Palma for genome analysis support and Sabrine Dhaouadi for assistance with data handling. The PpR24 genome sequence was done via the University of Exeter funded by the Wellcome Trust Institutional Strategic Support Fund (WT097835MF), Wellcome Trust Multi-User Equipment Award (WT101650MA), and the BBSRC LOLA award (BB/K003240/1).

FUNDING INFORMATION

D.P. was funded by the University of Reading and Bayer Crop Science. We acknowledge funding for M.R. and R. W.J. from BBSRC (BB/P006272/1) and a jointly funded grant from UKRI, Defra, and the Scottish Government, under the Strategic Priorities Fund Plant Bacterial Diseases programme (BB/T010568/1). T.H.M. acknowledges the BBSRC funded 'Growing Health' (BB/X010953/1) and 'Soils to Nutrition' (BBS/E/C/000I0310) Institute Strategic Programmes. An initial RNA seq experiment was carried out using the NERC Biomolecular Analysis Facility Liverpool via award NBAF794.

CONFLICT OF INTEREST STATEMENT

The authors declare no conflict of interest.

DATA AVAILABILITY STATEMENT

The datasets supporting the conclusions of this article are included within the article and its Appendix.

ORCID

Mojgan Rabiey https://orcid.org/0000-0001-8463-9087

REFERENCES

Abe, A. (2009) Bacterial secretion systems: their function and contribution to disease process. *Kansenshogaku Zasshi*, 83, 94–100.

Alsohim, A.S., Taylor, T.B., Barrett, G.A., Gallie, J., Zhang, X.X., Altamirano-Junqueira, A.E. et al. (2014) The biosurfactant viscosin produced by *Pseudomonas fluorescens* SBW25 aids spreading motility and plant growth promotion. *Environmental Microbiology*, 16, 2267–2281.

Amich, J., Schafferer, L., Haas, H. & Krappmann, S. (2013) Regulation of sulphur assimilation is essential for virulence and affects iron homeostasis of the human-pathogenic mould *Aspergillus fumigatus*. *PLoS Pathogens*, 9, e1003573.

Bahlai, C.A., Xue, Y., Mccreary, C.M., Schaafsma, A.W. & Hallett, R. H. (2010) Choosing organic pesticides over synthetic pesticides may not effectively mitigate environmental risk in soybeans. *PLoS One*, 5, e11250.

Bansal, R., Mian, M.A.R., Mittapalli, O. & Michel, A.P. (2014) RNA-Seq reveals a xenobiotic stress response in the soybean aphid, *Aphis glycines*, when fed aphid-resistant soybean. *BMC Genomics*, 15, 972.

Bass, C., Puinean, A.M., Zimmer, C.T., Denholm, I., Field, L.M., Foster, S.P. et al. (2014) The evolution of insecticide resistance in the peach potato aphid, *Myzus persicae*. *Insect Biochemistry and Molecular Biology*, 51, 41–51.

Basset, A., Tzou, P., Lemaitre, B. & Boccard, F. (2003) A single gene that promotes interaction of a phytopathogenic bacterium with its insect vector, *Drosophila melanogaster*. *EMBO Reports*, 4, 205–209.

Blackman R.L. & Eastop, E.L. (1994) *Aphids on the world's crops: an identification and information guide*, 2nd Edition, Wallingford: CAB International in association with the Natural History Museum.

Bowen, D., Rocheleau, T.A., Blackburn, M., Andreev, O., Golubeva, E., Bhartia, R. et al. (1998) Insecticidal toxins from the bacterium *Photorhabdus luminescens*. *Science*, 280, 2129–2132.

Boyd, E.F. & Hartl, D.L. (1998) Salmonella virulence plasmid. Modular acquisition of the spv virulence region by an F-plasmid in *Salmonella enterica* subspecies I and insertion into the chromosome of subspecies II, IIIa, IV and VII isolates. *Genetics*, 149, 1183–1190.

Bronstein, P.A., Filiatrault, M.J., Myers, C.R., Rutzke, M., Schneider, D.J. & Cartinhour, S.W. (2008) Global transcriptional responses of *Pseudomonas syringae* DC3000 to changes in iron bioavailability in vitro. *BMC Microbiology*, 8, 209.

Brugirard-Ricaud, K., Duchaud, E., Givaudan, A., Girard, P.A., Kunst, F., Boemare, N. et al. (2005) Site-specific antiphagocytic function of the *Photorhabdus luminescens* type III secretion system during insect colonization. *Cellular Microbiology*, 7, 363–371.

Casilag, F., Lorenz, A., Krueger, J., Klawonn, F., Weiss, S. & Häussler, S. (2015) The LasB elastase of *Pseudomonas aeruginosa* acts in concert with alkaline protease apra to prevent flagellin-mediated immune recognition. *Infection and Immunity*, 84, 162–171.

Chen, L., Zou, Y., She, P. & Wu, Y. (2015) Composition, function, and regulation of T6SS in *Pseudomonas aeruginosa*. *Microbiological Research*, 172, 19–25.

Choi, Y.S., Shin, D.H., Chung, I.Y., Kim, S.H., Heo, Y.J. & Cho, Y.H. (2007) Identification of *Pseudomonas aeruginosa* genes crucial for hydrogen peroxide resistance. *Journal of Microbiology and Biotechnology*, 17, 1344–1352.

Conesa, A. & Götz, S. (2008) Blast2GO: a comprehensive suite for functional analysis in plant genomics. *International Journal of Plant Genomics*, 2008, 619832.

Cornelis, P., Wei, Q., Andrews, S.C. & Vinckx, T. (2011) Iron homeostasis and management of oxidative stress response in bacteria. *Metallomics*, 3, 540–549.

Cornelissen, C.N. (2003) Transferrin-iron uptake by gram-negative bacteria. *Frontiers in Bioscience*, 8, d836–d847.

Correa, V.R., Majerczak, D.R., Ammar El, D., Merighi, M., Pratt, R.C., Hogenhout, S.A. et al. (2012) The bacterium *Pantoea stewartii* uses two different type III secretion systems to colonize its plant host and insect vector. *Applied and Environmental Microbiology*, 78, 6327–6336.

Costechareyre, D., Balmand, S., Condemine, G. & Rahbé, Y. (2012) *Dickeya dadantii*, a plant pathogenic bacterium producing Cyt-like entomotoxins, causes septicemia in the pea aphid *Acyrthosiphon pisum*. *PLoS One*, 7, e30702.

Cristofoletti, P.T., De Sousa, F.A.M., Rahbé, Y. & Terra, W.R. (2006) Characterization of a membrane-bound aminopeptidase purified from Acyrthosiphon pisum midgut cells. A major binding site for toxic mannose lectins. *The FEBS Journal*, 273, 5574–5588.

Cristofoletti, P.T., Ribeiro, A.F., Deraison, C., Rahbé, Y. & Terra, W. R. (2003) Midgut adaptation and digestive enzyme distribution in a phloem feeding insect, the pea aphid Acyrthosiphon pisum. *Journal of Insect Physiology*, 49, 11–24.

Davis, M.M. & Engström, Y. (2012) Immune response in the barrier epithelia: lessons from the fruit fly *Drosophila melanogaster*. *Journal of Innate Immunity*, 4, 273–283.

De Gregorio, E., Spellman, P.T., Rubin, G.M. & Lemaitre, B. (2001) Genome-wide analysis of the *Drosophila* immune response by using oligonucleotide microarrays. *Proceedings of the National Academy of Sciences of the United States of America*, 98, 12590–12595.

Dedryver, C.-A., Le Ralec, A. & Fabre, F. (2010) The conflicting relationships between aphids and men: a review of aphid damage and control strategies. *Comptes Rendus Biologies*, 333, 539–553.

Duchaud, E., Rusniok, C., Frangeul, L., Buchrieser, C., Givaudan, A., Taourit, S. et al. (2003) The genome sequence of the entomopathogenic bacterium *Photorhabdus luminescens*. *Nature Biotechnology*, 21, 1307–1313.

Dutta, S., Yu, S.M., Jeong, S.C. & Lee, Y.H. (2020) High-throughput analysis of genes involved in biocontrol performance of *Pseudomonas fluorescens* NBC275 against Gray mold. *Journal of Applied Microbiology*, 128, 265–279.

Filloux, A. (2011) Protein secretion systems in *Pseudomonas aeruginosa*: an essay on diversity, evolution, and function. *Frontiers in Microbiology*, 2, 155.

Flury, P., Aellen, N., Ruffner, B., Péchy-Tarr, M., Fataar, S., Metla, Z. et al. (2016) Insect pathogenicity in plant-beneficial pseudomonads: phylogenetic distribution and comparative genomics. *The ISME Journal*, 10, 2527–2542.

Flury, P., Vesga, P., Dominguez-Ferreras, A., Tinguely, C., Ullrich, C. I., Kleespies, R.G. et al. (2019) Persistence of root-colonizing *Pseudomonas protegens* in herbivorous insects throughout different developmental stages and dispersal to new host plants. *The ISME Journal*, 13, 860–872.

Flury, P., Vesga, P., Péchy-Tarr, M., Aellen, N., Dennert, F., Hofer, N. et al. (2017) Antimicrobial and insecticidal: cyclic lipopeptides and hydrogen cyanide produced by plant-beneficial pseudomonas strains CHA0, CMR12a, and PCL1391 contribute to insect killing. *Frontiers in Microbiology*, 8, 100.

Gallagher, L.A. & Manoil, C. (2001) Pseudomonas aeruginosa PAO1 kills *Caenorhabditis elegans* by cyanide poisoning. *Journal of Bacteriology*, 183, 6207–6214.

Garrido-Sanz, D., Vesga, P., Heiman, C.M., Altenried, A., Keel, C. & Vacheron, J. (2023) Relation of pest insect-killing and soilborne pathogen-inhibition abilities to species diversification in environmental *Pseudomonas protegens*. *The ISME Journal*, 17, 1369–1381.

Gerardo, N.M., Altincicek, B., Anselme, C., Atamian, H., Barribeau, S. M., De Vos, M. et al. (2010) Immunity and other defenses in pea aphids, *Acyrthosiphon pisum*. *Genome Biology*, 11, R21.

Gotoh, H., Okada, N., Kim, Y.-G., Shiraishi, K., Hirami, N., Haneda, T. et al. (2003) Extracellular secretion of the virulence plasmid-encoded ADP-ribosyltransferase SpvB in *Salmonella*. *Microbial Pathogenesis*, 34, 227–238.

Guo, J., Jing, X., Peng, W.-L., Nie, Q., Zhai, Y., Shao, Z. et al. (2016) Comparative genomic and functional analyses: unearthing the diversity and specificity of nematicidal factors in *Pseudomonas putida* strain 1A00316. *Scientific Reports*, 6, 29211.

Haas, D. & Défago, G. (2005) Biological control of soil-borne pathogens by fluorescent pseudomonads. *Nature Reviews Microbiology*, 3, 307–319.

Haas, D. & Keel, C. (2003) Regulation of antibiotic production in root-colonizing *Peudomonas* spp. and relevance for biological control of plant disease. *Annual Review of Phytopathology*, 41, 117–153.

Hassett, D.J., Howell, M.L., Sokol, P.A., Vasil, M.L. & Dean, G.E. (1997) Fumarase C activity is elevated in response to iron deprivation and in mucoid, alginate-producing *Pseudomonas aeruginosa*: cloning and characterization of fumC and purification of native fumC. *Journal of Bacteriology*, 179, 1442–1451.

Hillyer, J.F. (2016) Insect immunology and hematopoiesis. *Developmental and Comparative Immunology*, 58, 102–118.

Hou, Y.-J., Banerjee, R., Thomas, B., Nathan, C., García-Sastre, A., Ding, A. et al. (2013) SARM is required for neuronal injury and cytokine production in response to central nervous system viral infection. *Journal of Immunology (Baltimore, MD: 1950)*, 191, 875–883.

Horton, R.M., Cai, Z., Ho, S.M. & Pease, L.R. (1990) Gene splicing by overlap extension: tailor-made genes using the polymerase chain reaction. *Biotechniques*, 8(5), 528–535.

Huang, X., Dai, J., Fournier, J., Ali, A.M., Zhang, Q. & Frenkel, K. (2002) Ferrous ion autoxidation and its chelation in iron-loaded human liver HepG2 cells. *Free Radical Biology and Medicine*, 32, 84–92.

Irving, P., Troxler, L., Heuer, T.S., Belvin, M., Kopczynski, C., Reichhart, J.M. et al. (2001) A genome-wide analysis of immune responses in Drosophila. *Proceedings of the National Academy of Sciences of the United States of America*, 98, 15119–15124.

Jackson, A.P., Thomas, G.H., Parkhill, J. & Thomson, N.R. (2009) Evolutionary diversification of an ancient gene family (rhs) through C-terminal displacement. *BMC Genomics*, 10, 584.

Johnson, M., Zaretskaya, I., Raytselis, Y., Merezhuk, Y., Mcginnis, S. & Madden, T.L. (2008) NCBI BLAST: a better web interface. *Nucleic Acids Research*, 36, W5–W9.

Jousset, A., Rochat, L., Lanoue, A., Bonkowski, M., Keel, C. & Scheu, S. (2011) Plants respond to pathogen infection by enhancing the antifungal gene expression of root-associated bacteria. *Molecular Plant-Microbe Interactions*, 24, 352–358.

Kamilova, F., Validov, S., Azarova, T., Mulders, I. & Lugtenberg, B. (2005) Enrichment for enhanced competitive plant root tip colonizers selects for a new class of biocontrol bacteria. *Environmental Microbiology*, 7, 1809–1817.

Kammler, M., Schön, C. & Hantke, K. (1993) Characterization of the ferrous iron uptake system of *Escherichia coli*. *Journal of Bacteriology*, 175, 6212–6219.

Kang, Y.-S., Lee, Y., Jung, H., Jeon, C.O., Madsen, E.L. & Park, W. (2007) Overexpressing antioxidant enzymes enhances naphthalene biodegradation in *Pseudomonas* sp. strain As1. *Microbiology*, 153, 3246–3254.

Kawakami, T., Kuroki, M., Ishii, M., Igarashi, Y. & Arai, H. (2009) Differential expression of multiple terminal oxidases for aerobic respiration in *Pseudomonas aeruginosa*. *Environmental Microbiology*, 12(6), 1399–1412.

Keel, C. (2016) A look into the toolbox of multi-talents: insect pathogenicity determinants of plant-beneficial pseudomonads. *Environmental Microbiology*, 18, 3207–3209.

King, E.O., Ward, M.K. & Raney, D.E. (1954) Two simple media for the demonstration of pyocyanin and fluorescin. *The Journal of Laboratory and Clinical Medicine*, 44, 301–307.

Kunert, G. & Weisser, W.W. (2003) The interplay between density- and trait-mediated effects in predator-prey interactions: a case study in aphid wing polymorphism. *Oecologia*, 135, 304–312.

Kutsukake, M., Shibao, H., Nikoh, N., Morioka, M., Tamura, T., Hoshino, T. et al. (2004) Venomous protease of aphid soldier for colony defense. *Proceedings of the National Academy of Sciences of the United States of America*, 101, 11338–11343.

Langmead, B., Trapnell, C., Pop, M. & Salzberg, S.L. (2009) Ultrafast and memory-efficient alignment of short DNA sequences to the human genome. *Genome Biology*, 10, R25.

Liehl, P., Blight, M., Vodovar, N., Boccard, F. & Lemaitre, B. (2006) Prevalence of local immune response against oral infection in a *Drosophila*/*Pseudomonas* infection model. *PLoS Pathogens*, 2, e56.

Lim, C.K., Hassan, K.A., Tetu, S.G., Loper, J.E. & Paulsen, I.T. (2012) The effect of iron limitation on the transcriptome and proteome of *Pseudomonas fluorescens* Pf-5. *PLoS One*, 7, e39139.

Lin, X., Ruiz, J., Bajraktari, I., Ohman, R., Banerjee, S., Gribble, K. et al. (2014) Z-disc-associated, alternatively spliced, PDZ motif-containing protein (ZASP) mutations in the actin-binding domain cause disruption of skeletal muscle actin filaments in myofibrillar myopathy. *The Journal of Biological Chemistry*, 289, 13615–13626.

Liu, K., Knabel, S.J. & Dudley, E.G. (2009) rhs genes are potential markers for multilocus sequence typing of *Escherichia coli* O157:H7 strains. *Applied and Environmental Microbiology*, 75, 5853–5862.

Loper, J.E., Henkels, M.D., Rangel, L.I., Olcott, M.H., Walker, F.L., Bond, K.L. et al. (2016) Rhizoxin analogs, orfamide A and chitinase production contribute to the toxicity of *Pseudomonas protegens* strain Pf-5 to *Drosophila melanogaster*. *Environmental Microbiology*, 18, 3509–3521.

Lugtenberg, B. & Kamilova, F. (2009) Plant-growth-promoting rhizobacteria. *Annual Review of Microbiology*, 63, 541–556.

Ma, J.F., Ochsner, U.A., Klotz, M.G., Nanayakkara, V.K., Howell, M. L., Johnson, Z. et al. (1999) Bacterioferritin A modulates catalase A (KatA) activity and resistance to hydrogen peroxide in *Pseudomonas aeruginosa*. *Journal of Bacteriology*, 181, 3730–3742.

Marmaras, V.J., Bournazos, S.N., Katsoris, P.G. & Lambropoulou, M. (1993) Defense mechanisms in insects: certain integumental proteins and tyrosinase are responsible for nonself-recognition and immobilization of *Escherichia coli* in the cuticle of developing *Ceratitis capitata*. *Archives of Insect Biochemistry and Physiology*, 23, 169–180.

Mercado-Blanco, J. & Bakker, P.A. (2007) Interactions between plants and beneficial *Pseudomonas* spp.: exploiting bacterial traits for crop protection. *Antonie Van Leeuwenhoek*, 92, 367–389.

Merlin, C., Mcateer, S. & Masters, M. (2002) Tools for characterization of *Escherichia coli* genes of unknown function. *Journal of Bacteriology*, 184, 4573–4581.

Miller, J.H. (1972) *Experiments in molecular genetics*. Cold Spring Harbor: Cold Spring Harbor Laboratory.

Miyata, S., Casey, M., Frank, D.W., Ausubel, F.M. & Drenkard, E. (2003) Use of the *Galleria mellonella* caterpillar as a model host to study the role of the type III secretion system in *Pseudomonas aeruginosa* pathogenesis. *Infection and Immunity*, 71, 2404–2413.

Moir, M.L., Renton, M., Hoffmann, B.D., Leng, M.C. & Lach, L. (2018) Development and testing of a standardized method to estimate honeydew production. *PLoS One*, 13, e0201845.

Morel, V., Lepicard, S., Rey, A., Parmentier, M.-L. & Schaeffer, L. (2014) Drosophila Nesprin-1 controls glutamate receptor density at neuromuscular junctions. *Cellular and Molecular Life Sciences*, 71, 3363–3379.

Nappi, A.J. & Vass, E. (2000) Iron, metalloenzymes and cytotoxic reactions. *Cellular and Molecular Biology (Noisy-le-Grand, France)*, 46, 637–647.

Nehme, N.T., Liégeois, S., Kele, B., Giammarinaro, P., Pradel, E., Hoffmann, J.A. et al. (2007) A model of bacterial intestinal infections in *Drosophila melanogaster*. *PLoS Pathogens*, 3, e173.

Noinaj, N., Buchanan, S.K. & Cornelissen, C.N. (2012) The transferrin-iron import system from pathogenic *Neisseria* species. *Molecular Microbiology*, 86, 246–257.

Ochsner, U.A., Vasil, M.L., Alsabbagh, E., Parvatiyar, K. & Hassett, D.J. (2000) Role of the *Pseudomonas aeruginosa* oxyR-recG operon in oxidative stress defense and DNA repair: OxyR-dependent regulation of katB-ankb, ahpb, and ahpC-ahpF. *Journal of Bacteriology*, 182, 4533–4544.

Olcott, M.H., Henkels, M.D., Rosen, K.L., Walker, F.L., Sneh, B., Loper, J.E. et al. (2010) Lethality and developmental delay in *Drosophila melanogaster* larvae after ingestion of selected *Pseudomonas fluorescens* strains. *PLoS One*, 5, e12504.

Pal, S., Wu, J. & Wu, L.P. (2008) Microarray analyses reveal distinct roles for Rel proteins in the Drosophila immune response. *Developmental and Comparative Immunology*, 32, 50–60.

Paliwal, D., Hamilton, A.J., Barrett, G.A., Alberti, F., Van Emden, H., Monteil, C.L. et al. (2022) Identification of novel aphid-killing bacteria to protect plants. *Microbial Biotechnology*, 15, 1203–1220.

Palma, M., Worgall, S. & Quadri, L.E.N. (2003) Transcriptome analysis of the *Pseudomonas aeruginosa* response to iron. *Archives of Microbiology*, 180, 374–379.

Paulsen, I.T., Press, C.M., Ravel, J., Kobayashi, D.Y., Myers, G.S.A., Mavrodi, D.V. et al. (2005) Complete genome sequence of the plant commensal *Pseudomonas fluorescens* Pf-5. *Nature Biotechnology*, 23, 873–878.

Polack, B.T., Dacheux, D., Delic-Attree, I., Toussaint, B. & Vignais, P. M. (1996) The *Pseudomonas aeruginosa* fumcandsoda genes belong to an iron-responsive operon. *Biochemical and Biophysical Research Communications*, 226, 555–560.

Preston, G.M., Bertrand, N. & Rainey, P.B. (2001) Type III secretion in plant growth-promoting *Pseudomonas fluorescens* SBW25. *Molecular Microbiology*, 41, 999–1014.

Puca, L. & Brou, C. (2014) α-Arrestins – new players in Notch and GPCR signaling pathways in mammals. *Journal of Cell Science*, 127, 1359–1367.

Raaijmakers, J.M., De Bruijn, I., Nybroe, O. & Ongena, M. (2010) Natural functions of lipopeptides from Bacillusi and Pseudomonas: more than surfactants and antibiotics. *FEMS Microbiology Reviews*, 34, 1037–1062.

Rispe, C., Kutsukake, M., Doublet, V., Hudaverdian, S., Legeai, F., Simon, J.C. et al. (2007) Large gene family expansion and variable selective pressures for cathepsin B in aphids. *Molecular Biology and Evolution*, 25, 5–17.

Ruffner, B., Péchy-Tarr, M., Höfte, M., Bloemberg, G., Grunder, J., Keel, C. et al. (2015) Evolutionary patchwork of an insecticidal toxin shared between plant-associated pseudomonads and the insect pathogens Photorhabdus and Xenorhabdus. *BMC Genomics*, 16, 609.

Sapountzis, P., Duport, G., Balmand, S., Gaget, K., Jaubert-Possamai, S., Febvay, G. et al. (2014) New insight into the RNA interference response against cathepsin-L gene in the pea aphid, *Acyrthosiphon pisum*: molting or gut phenotypes specifically induced by injection or feeding treatments. *Insect Biochemistry and Molecular Biology*, 51, 20–32.

Sarwan, K. (2019) Aphid-plant interactions: implications for pest management. In: Manuel, T.O., Feyza, C. & Anabela, F.-S. (Eds.) *Plant communities and their environment*. Rijeka: IntechOpen.

Schmidt, M.H., Lauer, A., Purtauf, T., Thies, C., Schaefer, M. & Tscharntke, T. (2003) Relative importance of predators and parasitoids for cereal aphid control. *Proceedings of the Royal Society of London Series B–Biological Sciences*, 270, 1905–1909.

Spink, J.M., Pullinger, G.D., Wood, M.W. & Lax, A.J. (1994) Regulation of *spvr*, the positive regulatory gene of Salmonella plasmid virulence genes. *FEMS Microbiology Letters*, 116, 113–121.

Stavrinides, J., Mccloskey, J.K. & Ochman, H. (2009) Pea aphid as both host and vector for the phytopathogenic bacterium *Pseudomonas syringae*. *Applied and Environmental Microbiology*, 75, 2230–2235.

Stavrinides, J., No, A. & Ochman, H. (2010) A single genetic locus in the phytopathogen *Pantoea stewartiii* enables gut colonization and pathogenicity in an insect host. *Environmental Microbiology*, 12, 147–155.

Touati, D. (2000) Iron and oxidative stress in bacteria. *Archives of Biochemistry and Biophysics*, 373, 1–6.

Town, J., Cui, N., Audy, P., Boyetchko, S. & Dumonceaux, T.J. (2016) Improved high-quality draft genome sequence of *Pseudomonas fluorescens* KENGFT3. *Genome Announcements*, 4, e00428-16.

Trapnell, C., Williams, B.A., Pertea, G., Mortazavi, A., Kwan, G., Van Baren, M.J. et al. (2010) Transcript assembly and quantification by RNA-Seq reveals unannotated transcripts and isoform switching during cell differentiation. *Nature Biotechnology*, 28, 511–515.

Vacheron, J., Péchy-Tarr, M., Brochet, S., Heiman, C.M., Stojiljkovic, M., Maurhofer, M. et al. (2019) T6SS contributes to gut microbiome invasion and killing of an herbivorous pest insect by plant-beneficial *Pseudomonas protegens*. *The ISME Journal*, 13, 1318–1329.

Van Emden, H.F. & Wild, E.A. (2020) A fully defined artificial diet for Myzus persicae – the detailed technical manual. *Entomologia Experimentalis et Applicata*, 168, 582–586.

Vesga, P., Augustiny, E., Keel, C., Maurhofer, M. & Vacheron, J. (2021) Phylogenetically closely related pseudomonads isolated from arthropods exhibit differential insect-killing abilities and genetic variations in insecticidal factors. *Environmental Microbiology*, 23, 5378–5394.

Vesga, P., Flury, P., Vacheron, J., Keel, C., Croll, D. & Maurhofer, M. (2020) Transcriptome plasticity underlying plant root colonization and insect invasion by *Pseudomonas protegens*. *The ISME Journal*, 14, 2766–2782.

Vodovar, N., Vallenet, D., Cruveiller, S., Rouy, Z., Barbe, V., Acosta, C. et al. (2006) Complete genome sequence of the entomopathogenic and metabolically versatile soil bacterium *Pseudomonas entomophila*. *Nature Biotechnology*, 24, 673–679.

Vodovar, N., Vinals, M., Liehl, P., Basset, A., Degrouard, J., Spellman, P. et al. (2005) Drosophila host defense after oral infection by an entomopathogenic Pseudomonas species. *Proceedings of the National Academy of Sciences of the United States of America*, 102, 11414–11419.

Von Morgen, P., Hořejší, Z. & Macurek, L. (2015) Substrate recognition and function of the R2TP complex in response to cellular stress. *Frontiers in Genetics*, 6, 69.

Walker, K.A., Maltez, V.I., Hall, J.D., Vitko, N.P. & Miller, V.L. (2013) A phenotype at last: essential role for the *Yersinia enterocolitica* Ysa type III secretion system in a *Drosophila melanogaster* S2 cell model. *Infection and Immunity*, 81, 2478–2487.

Wang, L.F., Chai, L.Q., He, H.J., Wang, Q., Wang, J.X. & Zhao, X.F. (2010) A cathepsin L-like proteinase is involved in moulting and metamorphosis in *Helicoverpa armigera*. *Insect Molecular Biology*, 19, 99–111.

Waterfield, N.R., Bowen, D.J., Fetherston, J.D., Perry, R.D. & Ffrench-Constant, R.H. (2001) The tc genes of Photorhabdus: a growing family. *Trends in Microbiology*, 9, 185–191.

Waterhouse, R.M., Povelones, M. & Christophides, G.K. (2010) Sequence-structure-function relations of the mosquito leucine-rich repeat immune proteins. *BMC Genomics*, 11, 531.

Yan, Q., Philmus, B., Chang, J.H. & Loper, J.E. (2017) Novel mechanism of metabolic co-regulation coordinates the biosynthesis of secondary metabolites in *Pseudomonas protegens*. *eLife*, 6, e22835.

Yang, G. & Waterfield, N.R. (2013) The role of TcdB and TccC subunits in secretion of the Photorhabdus Tcd toxin complex. *PLoS Pathogens*, 9, e1003644.

Yao, H., Jepkorir, G., Lovell, S., Nama, P.V., Weeratunga, S., Battaile, K.P. et al. (2011) Two distinct ferritin-like molecules in Pseudomonas aeruginosa: the product of the bfrA gene is a bacterial ferritin (FtnA) and not a bacterioferritin (Bfr). *Biochemistry*, 50, 5236–5248.

Ye, X.-D., Su, Y.-L., Zhao, Q.-Y., Xia, W.-Q., Liu, S.-S. & Wang, X.-W. (2014) Transcriptomic analyses reveal the adaptive features and biological differences of guts from two invasive whitefly species. *BMC Genomics*, 15, 370.

Zerbino, D.R. (2010) Using the Velvet de novo assembler for short-read sequencing technologies. *Current Protocols in Bioinformatics* Chapter 11, Unit 11.5. https://doi.org/10.1002/0471250953.bi1105s31

SUPPORTING INFORMATION

Additional supporting information can be found online in the Supporting Information section at the end of this article.

How to cite this article: Paliwal, D., Rabiey, M., Mauchline, T.H., Hassani-Pak, K., Nauen, R., Wagstaff, C. et al. (2024) Multiple toxins and a protease contribute to the aphid-killing ability of *Pseudomonas fluorescens* PpR24. *Environmental Microbiology*, 26(4), e16604. Available from: https://doi.org/10.1111/1462-2920.16604

APPENDIX A

A.1 | METHODS AND RESULTS SECTION

A.1.1. | Evaluation of bacteria transcript inside treated aphid samples by real-time PCR method

To quantify bacterial transcripts inside aphids during the course of infection, quantitative PCR (qPCR) was employed to calculate the expression of bacteria mRNA levels in heterogeneous aphid–bacteria RNA samples. QPCR was conducted on aphid-treated cDNA samples after infection of bacteria at 12, 20, 24, and 36 h, and the amount of bacterial transcripts of PpR24 was measured using specific housekeeping and toxin primers. The results showed that no bacterial transcripts were recovered at the 12 h infection time but after 20 h of bacterial treatment, there was a constant increase in bacterial transcripts. Cycle threshold (Ct) values observed in qPCR reflect the bacterial cDNA levels with Ct values falling during the course of infection. These data helped identify the optimal infection time point for further RNA profiling experiments. After 38–40 h PpR24 infection, most aphids started melanisation, and 20%–30 % aphid death was observed in treated sachets. Hence, using a higher infection dose after 38 h to increase bacterial numbers would have increased the mortality of aphids. This would compromise the expression profiles obtained from aphids; therefore, 38 h was selected as optimal as up to this infection time point no aphid mortality was observed. To further increase the sequencing of bacterial transcripts in treated aphids an mRNA bacterial enrichment method in mixed aphid-bacteria RNA samples was used (see Section 2).

A.1.2. | Transcriptomic analysis methods

A.1.2.1. | Quality control and mapping of sequence reads

Quality control on raw sequence reads was performed using fastqc (http://www.bioinformatics.babraham.ac.uk/projects/fastqc/). The Illumina reads from the first RNA-Seq experiment required the additional step of trimming reads up to 80 bp which was done using the Galaxy software NGS tool; Trimmomatic-MILNEAN operation. The Galaxy software interface was used for further analysis. The paired-end sequencing forward and reverse reads of each replicate were mapped to the reference *Myzus persicae* Clone_G006 v1.0 (available at ArthropodaCyc metabolic database collection (http://arthropodacyc.cycadsys.org/)) and *Pseudomonas fluorescens* PpR24 genome (NCBI accession no: NIFJ00000000). To align the sequence reads to the respective genome, the TopHat tool (TopHat v2.1.0, http://tophat.cbcb.umd.edu/) with default parameters was used. All the reads were aligned to their respective genome using the efficient Bowtie aligner (Langmead et al., 2009), and then to find potential splice junctions between exons. The cufflinks (Trapnell et al., 2010) tool was used to assemble all transcripts into complete transcripts guided through the reference annotation file. It evaluates the relative abundance of assembled transcripts and was stated as fragments per kilobase of exon per million fragments mapped (FPKM) together with their confidence intervals. Each fragment resembles a single cDNA molecule, which can be signified by a pair of reads from each end. The Cufflinks tool was used to provide reference annotation to guide reference annotation-based transcript assembly. The final output file included all reference transcripts together with any novel assembled genes and isoforms. After assembling, all transcript replicates of both conditions were merged using the meta-assembler "Cuffmerge" (Trapnell et al., 2010). Furthermore, Cuffmerge performed Reference Annotation Based Transcript (RABT) assembly to merge reference transcripts with sample transcripts, which resulted in a single annotation file for use in differential gene analysis.

A.1.2.2. | Differential gene expression by Cuffdiff

Cuffdiff (Cuffdiff v2.2.1 (http://cufflinks.cbcb.umd.edu/)) was used to find transcripts exhibiting differential expression between different conditions (control and treated). In Cuffdiff the bias correction and multi-read correct option with reference genome were selected to avoid any artefacts. This tool calculates total read counts for each transcript across all replicates in each condition and further tested the significance of expressed transcripts in all replicates. Numerous output files (tabular output files) were generated by Cuffdiff as a result of differential gene expression between two conditions. Gene and transcript expression files comprise a common name and location in the genome and detailed statistical report of log2 FPKM, fold change (in log2 scale), and *p* values (both raw and adjusted for multiple testing using FDR). To examine only biologically relevant interesting gene changes, we selected more than 2-fold changes on differentially expressed (DE) genes with a cut-off *p* value of 0.05 for subsequent analysis.

A.1.3. | Differential expression analysis and data visualization

The transcripts from the samples were used for genome mapping, which showed the coverage of *M. persicae* in both control and treated conditions was ~89% in all replicates. All aphid-mapped transcripts were assembled by Cufflinks and merged by the assembler "Cuffmerge" to generate 18,400 genes with 32,184 transcripts. Similarly, all bacterial control replicates also showed 89 % mapped reads to the genome

although a lower mapping rate (~1%) was observed in treated, enriched mRNA of bacteria. A total of 4612 genes and 5467 transcripts were called after the assembly and merging of the bacterial transcriptome. Besides these, bacterial-treated reads were mapped to the *Buchnera* genome with 13% in all replicates. Due to the absence of control, *Buchnera-mapped* reads, no further transcriptomic analysis was conducted on these reads. The mapping results showed that all four aphid replicates of both conditions had more than 35 million reads mapped to the *M. persicae* genome, resulting in good RNA-Seq coverage as per guidelines (Lin et al., 2014). Similarly, bacterial control transcripts also represented excellent RNA-Seq coverage with more than 8 million reads.

Several quality control methods were employed to examine the fidelity of Cufflinks and Cuffdiff outputs. First, the variance between both treatment conditions and replicates was examined by a Multidimensional Scaling (MDS) plot (Figure S1). In the MDS plot, all biological replicates of control samples (both in aphid and bacteria) were assembled, signifying that low variation existed among the replicates. However, in the case of treated conditions (both in aphid and bacteria), three replicates clustered with small variations while a fourth replicate deviated from others. This variation might be the effect of treatment during infection (Figure S1). Moreover, the distribution of the FPKM values was also assessed by the CummeRbund tool that constructed a boxplot and csdensity of log10 transformed FPKM values for both conditions. There was an overall uniform distribution of log10 transformed FPKM values among conditions of both aphid and bacteria, signifying data were reproducible and high quality (Figures S2 and S3). The aphid Cufflinks datasets indicated average FPKM values among the conditions were close to 1 and slightly <1, suggesting that a high level of sequence coverage was allowed to identify low-expression genes. Importantly, the low number of reads in the treated bacterial sample did not bias the FPKM counts in regard to the control, hence a minimum cut-off FPKM value of 5 was used for subsequent analysis. Around 95% of genes in all replicates of treated bacteria consistently showed an FPKM of more than 10, which did not interfere with the differential gene analysis due to low sequence depth. Cufflinks and Cuffdiff estimated FPKMs for each transcript by summing all transcript counts associated with each gene to make an abundance metric for calculating DE at the gene level.

A.1.4. | Functional enrichment

Functional annotation is an effective approach to mining genomic data and uses statistical methods to find categorisation in functional classes (e.g., metabolic pathways, cellular processes, etc.). An updated annotation of both bacteria and aphid transcriptome was performed using the BLAST2GO (Blast2GO 3.3) platform. This involves searching genes against the GeneBank non-redundant database using BLASTx algorithms and implementing Gene Ontology (GO) annotation using the Swiss-Prot database and InterProScan (Conesa & Götz, 2008).

Further, functional enrichment analysis was done by Fisher's exact test to identify enriched biological functions in differentially expressed genes.